25. *The Vibration due to Obliquely Incident Waves of a Surface Stratum Adhering Closely to the Subjacent Medium, and the Properties of its Resonance Condition.*

By Genrokuro NISHIMURA and Takeo TAKAYAMA,

Earthquake Research Institute.

(Read Oct. 20, 1936—Received March 20, 1937.)

Introduction

In the previous paper[1] (in Japanese) one of the present writers discussed the vibratory motions of a surface layer and a subjacent semi-infinite elastic body when a dilatational wave is obliquely incident on the common boundary where the two solids adhere closely. The first chapter of that paper discussed the general properties of forced waves propagated in the two solids, namely, in the surface layer and in the subjacent solid when a dilatational wave of harmonic wave-type of infinite extent is obliquely incident on the bottom surface of the surface layer. In the second chapter were explained, analytically, the general phenomena of free wave-motions in the two solids when a dilatational wave of finite extent is obliquely incident on the common boundary.

The present paper, which is a continuation of the previous one, deals numerically, aided with numerous figures, with the case when a dilatational wave of harmonic type of infinite extent is obliquely incident on the bottom surface of the surface layer and the angle of incidence of this wave becomes 45°. From the mathematical results in the present paper, we obtained a number of facts helpful in studying the forced stationary vibrations of a particle in the surface layer of the earth's crust. We stated in the previous paper[2] that K. Sezawa[3] and K. Kanai have studied the forced wave-motions in the surface layer when a dilatational harmonic wave of infinite extent is obliquely incident upon the bottom surface of a surface layer and the angle of incidence of that wave becomes 45° as in the present paper. The elasticity conditions dealt with in their paper, however, differ somewhat from those

1) G. NISHIMURA, *Bull. Earthq. Res. Inst.*, **13** (1935), 540~554.
2) G. NISHIMURA, *loc. cit.*
3) K. SEZAWA and K. KANAI, *Bull. Earthq. Res. Inst.*, **10** (1932), 806; **12** (1934), 269.

treated in the present paper, namely, that whereas the ratio of rigidity of the surface stratum to that of the subjacent medium is 1/2 in Sezawa's case, in the present paper it is 1/10 for the purpose of theoretically investigating the seismal oscillation of the ground at Marunouti, a ground typifying the down-town of Tokyo.

In recent years the predominating periods of seismic oscillations of various grounds have been studied experimentally by M. Ishimoto[4], T. Saita[5], and W. Inouye[6]. Their views of the seismal oscillations of a surface layer of the earth's crust involve the assumption that the surface layer may be treated as an isolated elastic pendulum, the subjacent medium having no relation to the vibration in the surface layer. This theory seems to be supported in particular by the results[7] of analysis of the seismic acceleration of the ground at Marunouti. Sezawa[8], who has mathematically studied the vibrations of a surface stratum when elastic waves of infinite and finite extent are incident vertically upward on the bottom surface of the surface layer, shows that it is not satisfactory, in dealing with the seismal vibrations of the surface stratum, to assume that the stratum is an isolated body, as we do in the case of an elastic pendulum. He also extended his theory to enable comparison of his mathematical results with the actual facts[9] as learned from the seismometrical observations at Marunouti.

As already mentioned, we shall study in the present paper the forced stationary oscillations of the surface layer when harmonic waves of infinite extent are obliquely incident on the bottom surface of the surface layer. For this reason it will not be possible for us to explain from the results in the present paper the existence of predominating periods of seismal oscillations in the surface layer, which may result from the seismal vibrations of the surface layer due to free seismic waves propagated in the surface layer, although we shall be able to explain satisfactorily the existence of resonance periods of vibration in the surface layer. The former we shall no doubt be able to explain upon carefully studying the mathematical results contained in the second chapter[10] of the preceding paper.

4) M. ISHIMOTO, *Bull. Earthq. Res. Inst.*, **9** (1931), 316; **9** (1931), 473; **10** (1932), 171; **12** (1934), 234.
5) T. SAITA and M. SUZUKI, *Bull. Earthq. Res. Inst.*, **12** (1934), 517.
6) W. INOUYE, *Bull. Earthq. Res. Inst.*, **12** (1934), 712.
7) T. SAITA and M. SUZUKI, *loc. cit.*
8) K. SEZAWA, *Bull. Earthq. Inst.*, **8** (1930), 1.
K. SEZAWA and K. KANAI, *Bull. Earthq. Res. Inst.*, **13** (1635), 251.
9) T. SAITA and M. SUZUKI, *loc. cit.*
10) G. NISHIMURA, *loc. cit.*

Chapter I. Bodily Waves in a Semi-infinite Solid having a Surface Layer When a Dilatational Harmonic Wave of Infinite Extent is Obliquely Incident on the Common Boundary of These Two Solids where They Adhere Closely.

1. *General Solutions.*

Let the horizontal boundary of a surface layer of thickness H and a subjacent medium be $y=0$, and let the axis of x be on this common boundary, the axis of y being drawn vertically downward and positive, as shown in Fig. 1. Again let ρ and λ, μ be the density and Lame's elastic constants of the subjacent medium $y\geqq 0$ and ρ', and λ', μ' those of the surface layer.

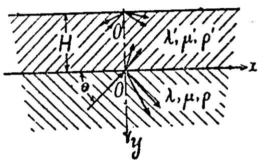

Fig. 1.

If the primary incident wave in the subjacent medium $y\geqq 0$ be of the type

$$\phi_0=\alpha e^{i(fx-ry-pt)}, \tag{1}$$

where α is a constant representing the intensity of this wave; and $p=2\pi/T$, where T is the period of this incident harmonic wave; and $r^2=\{\rho p^2/(\lambda+2\mu)\}-f^2$, obviously, f will depend on the wave-length L and the emergent angle θ of this wave. When the primary wave expressed by (1) is incident on the bottom surface of the surface layer, the following two waves are reflected at the common boundary in the subjacent medium $y\geqq 0$,

$$\phi=Ae^{i(fx+ry-pt)}, \tag{2}$$

$$\psi=Be^{i(fx+sy-pt)}, \tag{3}$$

where ϕ is the reflected dilatational wave and ψ the reflected distortional wave, both of which respectively satisfy the wave equations

$$\frac{\partial^2\phi}{\partial t^2}=\frac{\lambda+2\mu}{\rho}\nabla^2\phi, \tag{4}$$

$$\frac{\partial^2\psi}{\partial t^2}=\frac{\mu}{\rho}\nabla^2\psi. \tag{5}$$

In expressions (2), (3), A and B are arbitrary constants to be determined from the boundary conditions at $y=0$ and $y=-H$, and $s^2=\rho p^2/\mu-f^2$. Naturally wave expression (1) satisfies wave equation (4).

Let the refracted and reflected waves in the surface layer due to the incidence of the primary wave (1) be expressed by

$$\phi' = Ce^{i(fx - r'y - pt)} + De^{i(fx + r'y - pt)}, \tag{6}$$

$$\psi' = Ee^{i(fx - s'y - pt)} + Fe^{i(fx + s'y - pt)}, \tag{7}$$

where C and E are respectively intensities of the refracted dilatational and distortional waves to be determined, and also D, F those of the dilatational and distortional waves reflected at the free surface of the layer $y = -H$; and let $r'^2 = \rho' p^2 / (\lambda' + 2\mu') - f^2$, $s'^2 = \rho' p^2 / \mu' - f^2$ respectively. Obviously, ϕ' and ψ' satisfy the following wave equations in the surface layer:

$$\frac{\partial^2 \phi'}{\partial t^2} = \frac{\lambda' + 2\mu'}{\rho'} \Gamma^2 \phi', \tag{8}$$

$$\frac{\partial^2 \psi'}{\partial t^2} = \frac{\mu'}{\rho'} \Gamma^2 \psi'. \tag{9}$$

Let U' and V' be the horizontal and vertical movements of the particle in the surface layer respectively, and U and V be those in the subjacent medium, when we shall then be able to obtain these movements from (6), (7) and (1), (2), (3) respectively. Now we can easily obtain the horizontal and the vertical displacements (u_0, v_0) of a particle due to the incident primary wave (1) as follows:

$$\left.\begin{aligned} u_0 &= ifae^{i(fx - ry - pt)}, \\ v_0 &= -irae^{i(fx - ry - pt)}. \end{aligned}\right\} \tag{10}$$

The horizontal and vertical movements in the lower medium $y \geqq 0$ due to waves ϕ and ψ are respectively given by

$$\left.\begin{aligned} u_1 &= ifAe^{i(fx + ry - pt)}, \\ v_1 &= irAe^{i(fx + ry - pt)}, \end{aligned}\right\} \tag{11}$$

$$\left.\begin{aligned} u_2 &= isBe^{i(fx + sy - pt)}, \\ u_2 &= -ifBe^{i(fx + sy - pt)}, \end{aligned}\right\} \tag{12}$$

those in the surface layer due to waves ϕ' and ψ' being expressed by

$$\left.\begin{aligned} u_1' &= ifCe^{i(fx - r'y - pt)} + ifDe^{i(fx + r'y - pt)}, \\ v_1' &= -ir'Ce^{i(fx - r'y - pt)} + ir'De^{i(fx + r'y - pt)}, \end{aligned}\right\} \tag{13}$$

$$\left.\begin{aligned} u_2' &= -is'Ee^{i(fx-s'y-pt)}+is'Fe^{i(fx+s'y-pt)}, \\ v_2' &= -ifEe^{i(fx-s'y-pt)}-ifFe^{i(fx+s'y-pt)}. \end{aligned}\right\} \tag{14}$$

We then get the expressions

$$U=u_0+u_1+u_2, \qquad V=v_0+v_1+v_2,$$

$$U'=u_1'+u_2', \qquad V'=v_1'+v_2',$$

or

$$U=if\mathfrak{a}e^{i(fx-ry-pt)}+ifAe^{i(fx+ry-pt)}+isBe^{i(fx+sy-pt)}, \tag{15}$$

$$V=-ir\mathfrak{a}e^{i(fx-ry-pt)}+irAe^{i(fx+ry-pt)}-ifBe^{i(fx+sy-pt)}, \tag{16}$$

$$U'=ifCe^{i(fx-r'y-pt)}+ifDe^{i(fx+r'y-pt)}-is'Ee^{i(fx-s'y-pt)}+is'Fe^{i(fx+s'y-pt)}, \tag{17}$$

$$V'=-ir'Ce^{i(fx-r'y-pt)}+ir'De^{i(fx+r'y-pt)}-ifEe^{i(fx-s'y-pt)}-ifFe^{i(fx+s'y-pt)}. \tag{18}$$

The conditions in which the displacements and the stresses of both solids are continuous at the common boundary $y=0$ are analytically expressed by

$$\left.\begin{aligned} &U=U', \qquad V=V', \\ &\lambda\left(\frac{\partial U}{x}+\frac{\partial V}{\partial y}\right)+2\mu\frac{\partial V}{\partial y}=\lambda'\left(\frac{\partial U'}{\partial x}+\frac{\partial V'}{\partial y}\right)+2\mu'\frac{\partial V'}{\partial y}, \\ &\mu\left(\frac{\partial V}{\partial x}+\frac{\partial U}{\partial y}\right)=\mu'\left(\frac{\partial V'}{\partial x}+\frac{\partial U'}{\partial y}\right), \end{aligned}\right\} \tag{19}$$

and the conditions in which the top surface of the surface layer $y=-H$ is a free surface are also expressed by

$$\left.\begin{aligned} &\lambda'\left(\frac{\partial U'}{\partial x}+\frac{\partial V'}{\partial y}\right)+2\mu'\frac{\partial V'}{\partial y}=0, \\ &\mu'\left(\frac{\partial V'}{\partial x}+\frac{\partial U'}{\partial y}\right)=0. \end{aligned}\right\} \tag{20}$$

We obtain the following values of A, B, C, D, E, and F thus determined from conditions (19), (20)

$$\left.\begin{aligned} A&=\frac{\Delta_A}{\Delta}\mathfrak{a}, \qquad B=\frac{\Delta_B}{\Delta}\mathfrak{a}, \qquad C=\frac{\Delta_C}{\Delta}\mathfrak{a}, \\ D&=\frac{\Delta_D}{\Delta}\mathfrak{a}, \qquad E=\frac{\Delta_E}{\Delta}\mathfrak{a}, \qquad F=\frac{\Delta_F}{\Delta}\mathfrak{a}, \end{aligned}\right\} \tag{21}$$

where

$$\Delta=16\frac{r's'}{f^2}\left(1-\frac{s'^2}{f^2}\right)\left[-\mu^2\left\{\left(1-\frac{s^2}{f^2}\right)^2+4\frac{rs}{f^2}\right\}+\mu\mu'\left(1-\frac{s^2}{f^2}+2\frac{rs}{f^2}\right)\left(3-\frac{s'^2}{f^2}\right)\right.$$

$$\left.-2\mu'^2\left(1+\frac{rs}{f^2}\right)\left(1-\frac{s'^2}{f^2}\right)\right]$$

$$+e^{i(r'+s')H}\left\{\left(1-\frac{s'^2}{f^2}\right)^2+4\frac{r's'}{f^2}\right\}\left[\mu^2\left(1+\frac{r's'}{f^2}\right)\left\{\left(1-\frac{s^2}{f^2}\right)^2+4\frac{rs}{f^2}\right\}\right.$$

$$-\mu\mu'\left\{\left(1+\frac{s^2}{f^2}\right)\left(1+\frac{s'^2}{f^2}\right)\left(\frac{sr'}{f^2}+\frac{rs'}{f^2}\right)+2\left(1-\frac{s^2}{f^2}+2\frac{rs}{f^2}\right)\left(1-\frac{s'^2}{f^2}+2\frac{r's'}{f^2}\right)\right\}$$

$$\left.+\mu'^2\left(1+\frac{rs}{f^2}\right)\left\{\left(1-\frac{s'^2}{f^2}\right)^2+4\frac{r's'}{f^2}\right\}\right]$$

$$+e^{i(r'-s')H}\left\{\left(1-\frac{s'^2}{f^2}\right)^2-4\frac{r's'}{f^2}\right\}\left[-\mu^2\left(1-\frac{r's'}{f^2}\right)\left\{\left(1-\frac{s^2}{f^2}\right)^2+4\frac{rs}{f^2}\right\}\right.$$

$$+\mu\mu'\left\{\left(1+\frac{s^2}{f^2}\right)\left(1+\frac{s'^2}{f^2}\right)\left(\frac{sr'}{f^2}-\frac{rs'}{f^2}\right)+2\left(1-\frac{s^2}{f^2}+2\frac{rs}{f^2}\right)\left(1-\frac{s'^2}{f^2}-2\frac{r's'}{f^2}\right)\right\}$$

$$\left.-\mu'^2\left(1+\frac{rs}{f^2}\right)\left\{\left(1-\frac{s'^2}{f^2}\right)^2-4\frac{r's'}{f^2}\right\}\right]$$

$$+e^{-i(r'-s')H}\left\{\left(1-\frac{s'^2}{f^2}\right)^2-4\frac{r's'}{f^2}\right\}\left[-\mu^2\left(1-\frac{r's'}{f^2}\right)\left\{\left(1-\frac{s^2}{f^2}\right)^2+4\frac{rs}{f^2}\right\}\right.$$

$$+\mu\mu'\left\{2\left(-\frac{s^2}{f^2}+2\frac{rs}{f^2}\right)\left(1-\frac{s'^2}{f^2}-2\frac{r's'}{f^2}\right)+\left(1+\frac{s^2}{f^2}\right)\left(1+\frac{s'^2}{f^2}\right)\left(\frac{rs'}{f^2}-\frac{r's}{f^2}\right)\right\}$$

$$\left.-\mu'^2\left(1+\frac{rs}{f^2}\right)\left\{\left(1-\frac{s'^2}{f^2}\right)^2-4\frac{r's'}{f^2}\right\}\right]$$

$$+e^{-i(r'+s')H}\left\{\left(1-\frac{s'^2}{f^2}\right)^2+4\frac{r's'}{f^2}\right\}\left[\mu^2\left(1+\frac{r's'}{f^2}\right)\left\{\left(1-\frac{s^2}{f^2}\right)^2+4\frac{rs}{f^2}\right\}\right.$$

$$+\mu\mu'\left\{\left(1+\frac{s^2}{f^2}\right)\left(1+\frac{s'^2}{f^2}\right)\left(\frac{rs'}{f^2}+\frac{sr'}{f^2}\right)-2\left(1-\frac{s^2}{f^2}+2\frac{rs}{f^2}\right)\left(1-\frac{s'^2}{f^2}+2\frac{r's'}{f^2}\right)\right\}$$

$$\left.+\mu'^2\left(1+\frac{rs}{f^2}\right)\left\{\left(1-\frac{s'^2}{f^2}\right)^2+4\frac{r's'}{f^2}\right\}\right], \qquad (22)$$

$$
\begin{aligned}
\varDelta_A = 16\frac{r's'}{f^2}\left(1-\frac{s'^2}{f^2}\right)&\left[\mu^2\left\{1\left(-\frac{s^2}{f^2}\right)^2-4\frac{rs}{f^2}\right\}-\mu\mu'\left(1-\frac{s^2}{f^2}-2\frac{rs}{f^2}\right)\left(3-\frac{s'^2}{f^2}\right)\right.\\
&\left.\quad+2\mu'^2\left(1-\frac{rs}{f^2}\right)\left(1-\frac{s'^2}{f^2}\right)\right]\\
+e^{i(r'+s')H}\left\{\left(1-\frac{s'^2}{f^2}\right)^2+4\frac{r's'}{f^2}\right\}&\left[-\mu^2\left(1+\frac{r's'}{f^2}\right)\left\{\left(1-\frac{s^2}{f^2}\right)^2-4\frac{rs}{f^2}\right\}\right.\\
&+\mu\mu'\left\{\left(1+\frac{s^2}{f^2}\right)\left(1+\frac{s'^2}{f^2}\right)\left(\frac{r's}{f^2}-\frac{rs'}{f^2}\right)+2\left(1-\frac{s^2}{f^2}-2\frac{rs}{f^2}\right)\left(1-\frac{s'^2}{f^2}+2\frac{r's'}{f^2}\right)\right\}\\
&\left.-\mu'^2\left(1-\frac{rs}{f^2}\right)\left\{\left(1-\frac{s'^2}{f^2}\right)^2+4\frac{r's'}{f^2}\right\}\right]\\
+e^{i(r'-s')H}\left\{\left(1-\frac{s'^2}{f^2}\right)^2-4\frac{r's'}{f^2}\right\}&\left[\mu^2\left(1-\frac{r's'}{f^2}\right)\left\{\left(1-\frac{s^2}{f^2}\right)^2-4\frac{rs}{f^2}\right\}\right.\\
&-\mu\mu'\left\{\left(1+\frac{s^2}{f^2}\right)\left(1+\frac{s'^2}{f^2}\right)\left(\frac{sr'}{f^2}+\frac{rs'}{f^2}\right)+2\left(1-\frac{s^2}{f^2}-2\frac{rs}{f^2}\right)\left(1-\frac{s'^2}{f^2}-2\frac{r's'}{f^2}\right)\right\}\\
&\left.+\mu'^2\left(1-\frac{rs}{f^2}\right)\left\{\left(1-\frac{s'^2}{f^2}\right)^2-4\frac{r's'}{f^2}\right\}\right]\\
+e^{-i(r'+s')H}\left\{\left(1-\frac{s'^2}{f^2}\right)^2+4\frac{r's'}{f^2}\right\}&\left[-\mu^2\left(1+\frac{r's'}{f^2}\right)\left\{\left(1-\frac{s^2}{f^2}\right)^2-4\frac{rs}{f^2}\right\}\right.\\
&+\mu\mu'\left\{\left(1+\frac{s^2}{f^2}\right)\left(1+\frac{s'^2}{f^2}\right)\left(\frac{rs'}{f^2}-\frac{r's}{f^2}\right)+2\left(1-\frac{s^2}{f^2}-2\frac{rs}{f^2}\right)\left(1-\frac{s'^2}{f^2}+2\frac{r's'}{f^2}\right)\right\}\\
&\left.-\mu'^2\left(1-\frac{rs}{f^2}\right)\left\{\left(1-\frac{s'^2}{f^2}\right)^2+4\frac{r's'}{f^2}\right\}\right]\\
+e^{-i(r'-s')H}\left\{\left(1-\frac{s'^2}{f^2}\right)^2-4\frac{r's'}{f^2}\right\}&\left[\mu^2\left(1-\frac{r's'}{f^2}\right)\left\{\left(1-\frac{s^2}{f^2}\right)^2-4\frac{rs}{f^2}\right\}\right.\\
&+\mu\mu'\left\{\left(1+\frac{s^2}{f^2}\right)\left(1+\frac{s'^2}{f^2}\right)\left(\frac{r's}{f^2}+\frac{rs'}{f^2}\right)-2\left(1-\frac{s^2}{f^2}-2\frac{rs}{f^2}\right)\left(1-\frac{s'^2}{f^2}-2\frac{r's'}{f^2}\right)\right\}\\
&\left.+\mu'^2\left(1-\frac{rs}{f^2}\right)\left\{\left(1-\frac{s'^2}{f^2}\right)^2-4\frac{r's'}{f^2}\right\}\right], \qquad (23)
\end{aligned}
$$

$$\begin{aligned}
\Delta_R = {} & 16\frac{rr's'}{f^3}\left(1-\frac{s'^2}{f^2}\right)\left[4\mu^2\left(1-\frac{s^2}{f^2}\right)-\mu\mu'\left(3-\frac{s^2}{f^2}\right)\left(3-\frac{s'^2}{f^2}\right)+4\mu'^2\left(1-\frac{s'^2}{f^2}\right)\right] \\
& +2e^{i(r'+s')H}\frac{r}{f}\left\{\left(1-\frac{s'^2}{f^2}\right)^2+4\frac{r's'}{f^2}\right\}\left[-2\mu^2\left(1-\frac{s^2}{f^2}\right)\left(1+\frac{r's'}{f^2}\right)\right. \\
& \qquad \left.+\mu\mu'\left(3-\frac{s^2}{f^2}\right)\left(1-\frac{s'^2}{f^2}+2\frac{r's'}{f^2}\right)-\mu'^2\left\{\left(1-\frac{s'^2}{f^2}\right)^2+4\frac{r's'}{f^2}\right\}\right] \\
& +2e^{i(r'-s')H}\frac{r}{f}\left\{\left(1-\frac{s'^2}{f^2}\right)^2-4\frac{r's'}{f^2}\right\}\left[2\mu^2\left(1-\frac{s^2}{f^2}\right)\left(1-\frac{r's'}{f^2}\right)\right. \\
& \qquad \left.-\mu\mu'\left(3-\frac{s^2}{f^2}\right)\left(1-\frac{s'^2}{f^2}-2\frac{r's'}{f^2}\right)+\mu'^2\left\{\left(1-\frac{s'^2}{f^2}\right)^2-4\frac{r's'}{f^2}\right\}\right] \\
& +2e^{-i(r'+s')H}\frac{r}{f}\left\{\left(1-\frac{s'^2}{f^2}\right)^2+4\frac{r's'}{f^2}\right\}\left[-2\mu^2\left(1-\frac{s^2}{f^2}\right)\left(1+\frac{r's'}{f^2}\right)\right. \\
& \qquad \left.+\mu\mu'\left(3-\frac{s^2}{f^2}\right)\left(1-\frac{s'^2}{f^2}+2\frac{r's'}{f^2}\right)-\mu'^2\left\{\left(1-\frac{s'^2}{f^2}\right)^2+4\frac{r's'}{f^2}\right\}\right] \\
& +2e^{-i(r'-s')H}\frac{r}{f}\left\{\left(1-\frac{s'^2}{f^2}\right)^2-4\frac{r's'}{f^2}\right\}\left[2\mu^2\left(1-\frac{s^2}{f^2}\right)\left(1-\frac{r's'}{f^2}\right)\right. \\
& \qquad \left.-\mu\mu'\left(3-\frac{s^2}{f^2}\right)\left(1-\frac{s'^2}{f^2}-2\frac{r's'}{f^2}\right)+\mu'^2\left\{\left(1-\frac{s'^2}{f^2}\right)^2-4\frac{r's'}{f^2}\right\}\right],
\end{aligned} \tag{24}$$

$$\begin{aligned}
\Delta_C = {} & 8\frac{rs'}{f^2}\left(1+\frac{s^2}{f^2}\right)\left(1-\frac{s'^2}{f^2}\right)\left[-\mu^2\left(2\frac{r's}{f^2}-1+\frac{s^2}{f^2}\right)+\mu\mu'\left(2\frac{r's}{f^2}-1+\frac{s'^2}{f^2}\right)\right] \\
& +2e^{-i(r'-s')H}\frac{r}{f}\left(1+\frac{s^2}{f^2}\right)\left\{\left(1-\frac{s'^2}{f^2}\right)^2-4\frac{r's'}{f^2}\right\} \\
& \qquad \cdot\left[\mu\mu'\left\{\frac{s}{f}\left(1-\frac{s'^2}{f^2}\right)+2\frac{s'}{f}\right\}-\mu^2\left\{\frac{s'}{f}\left(1-\frac{s^2}{f^2}\right)+2\frac{s}{f}\right\}\right] \\
& +2e^{-i(r'+s')H}\frac{r}{f}\left(1+\frac{s^2}{f^2}\right)\left\{\left(1-\frac{s'^2}{f^2}\right)^2+4\frac{r's'}{f^2}\right\} \\
& \qquad \cdot\left[\mu\mu'\left\{-\frac{s}{f}\left(1-\frac{s'^2}{f^2}\right)+2\frac{s'}{f}\right\}+\mu^2\left\{-\frac{s'}{f}\left(1-\frac{s^2}{f^2}\right)+2\frac{s}{f}\right\}\right],
\end{aligned} \tag{25}$$

$$
\begin{aligned}
\varDelta_D = & 8\frac{rs'}{f^2}\left(1+\frac{s^2}{f^2}\right)\left(1-\frac{s'^2}{f^2}\right)\left[-\mu^2\left\{2\frac{r's}{f^2}+1-\frac{s^2}{f^2}\right\}+\mu\mu'\left\{2\frac{r's}{f^2}+1-\frac{s'^2}{f^2}\right\}\right] \\
& +2e^{i(r'+s')H}\frac{r}{f}\left(1+\frac{s^2}{f^2}\right)\left\{\left(1-\frac{s'^2}{f^2}\right)^2+4\frac{r's'}{f^2}\right\} \\
& \cdot\left[-\mu\mu'\left\{\frac{s}{f}\left(1-\frac{s'^2}{f^2}\right)+2\frac{s'}{f}\right\}+\mu^2\left\{\frac{s'}{f}\left(1-\frac{s^2}{f^2}\right)+2\frac{s}{f}\right\}\right] \\
& +2e^{i(r'-s')H}\frac{r}{f}\left(1+\frac{s^2}{f^2}\right)\left\{\left(1-\frac{s'^2}{f^2}\right)^2-4\frac{r's'}{f^2}\right\} \\
& \cdot\left[\mu\mu'\left\{\frac{s}{f}\left(1-\frac{s'^2}{f^2}\right)-2\frac{s'}{f}\right\}+\mu^2\left\{\frac{s'}{f}\left(1-\frac{s^2}{f^2}\right)-2\frac{s}{f}\right\}\right],
\end{aligned} \tag{26}
$$

$$
\begin{aligned}
\varDelta_E = & 8\frac{rr'}{f^2}\left(1+\frac{s^2}{f^2}\right)\left(1-\frac{s'^2}{f^2}\right)\left[\mu^2\left\{\frac{s'}{f}\left(1-\frac{s^2}{f^2}\right)+2\frac{s}{f}\right\}-\mu\mu'\left\{\frac{s}{f}\left(1-\frac{s'^2}{f^2}\right)+2\frac{s'}{f^2}\right)\right] \\
& +2e^{-i(r'+s')H}\frac{r}{f}\left(1+\frac{s^2}{f^2}\right)\left\{\left(1-\frac{s'^2}{f^2}\right)^2+4\frac{r's'}{f^2}\right\} \\
& \cdot\left[\mu\mu'\left(1-\frac{s'^2}{f^2}+2\frac{r's}{f^2}\right)-\mu^2\left(1-\frac{s^2}{f^2}+2\frac{r's}{f^2}\right)\right] \\
& +2e^{i(r'-s')H}\frac{r}{f}\left(1+\frac{s^2}{f^2}\right)\left\{\left(1-\frac{s'^2}{f^2}\right)^2-4\frac{r's'}{f^2}\right\} \\
& \cdot\left[-\mu\mu'\left(1-\frac{s'^2}{f^2}-2\frac{r's}{f^2}\right)+\mu^2\left(1-\frac{s^2}{f^2}-2\frac{r's}{f^2}\right)\right],
\end{aligned} \tag{27}
$$

$$
\begin{aligned}
\varDelta_F = & 8\frac{rr'}{f^2}\left(1+\frac{s^2}{f^2}\right)\left(1-\frac{s'^2}{f^2}\right)\left[\mu^2\left\{\frac{s'}{f}\left(1-\frac{s^2}{f^2}\right)-2\frac{s}{f}\right\}+\mu\mu'\left\{\frac{s}{f}\left(1-\frac{s'^2}{f^2}\right)-2\frac{s'}{f}\right\}\right] \\
& +2e^{i(r'+s')H}\frac{r}{f}\left(1+\frac{s^2}{f^2}\right)\left\{\left(1-\frac{s'^2}{f^2}\right)^2+4\frac{r's'}{f^2}\right\} \\
& \cdot\left[\mu\mu'\left(1-\frac{s'^2}{f^2}-2\frac{r's}{f^2}\right)-\mu^2\left(1-\frac{s^2}{f^2}-2\frac{r's}{f^2}\right)\right] \\
& +2e^{-i(r'-s')H}\frac{r}{f}\left(1+\frac{s^2}{f^2}\right)\left\{\left(1-\frac{s'^2}{f^2}\right)^2-4\frac{r's'}{f^2}\right\} \\
& \cdot\left[-\mu\mu'\left(1-\frac{s'^2}{f^2}+2\frac{r's}{f^2}\right)+\mu^2\left(1-\frac{s^2}{f^2}+2\frac{r's}{f}\right)\right],
\end{aligned} \tag{28}
$$

It will be seen that the constants A, B, C, D, E, F thus determined usually become complex values, being transcendental functions, the variables of which are composed of the emergent angle θ and the wave-length L of the primary wave (1), and also the densities, the elastic constants of both media, and naturally the thickness of the surface layer H. Now each orbital motion of a particle in both media due to the seven waves expressed by (1), (2), (3), (6), and (7) is simple-harmonic, the orbit of which becomes a straight line. The amplitude and phase-differance of this simple-harmonic motion are transcendental functions having the same variables as the six constants A, B, C, D, E, and F. For these reasons every particle in both media (the surface layer and the subjacent medium) generally pursue elliptic orbital motions. The major and minor axes of the elliptic orbits and the inclination angle which the major axis makes with the horizontal surface are also transcendental functions, the variables of which are composed of θ, L, H, ρ, ρ', λ, μ, λ', μ'. We shall now study an example in which $\rho=\rho'$, $\lambda=\mu$, $\lambda'=\mu'$, $\mu'/\mu=1/10$[11] and the emergent angle of the primary wave $\theta=45°$. We then get the following expressions of Δ, Δ_A, Δ_B, Δ_C, Δ_D, Δ_E, and Δ_F in order to determine A, B, C, D, E, F:

$$\Delta=740496+6802609\cos(r'+s')H+4482215\cos(r'-s')H$$
$$-i4388760\sin(r'+s')H+i480220\sin(r'-s')H, \quad (29)$$

$$\Delta_A=1210195-1505732\cos(r'+s')H-3106149\cos(r'-s')H$$
$$+i520046\sin(r'+s')H-i4052695\sin(r'-s')H, \quad (30)$$

$$\Delta_B=917154+3344876\cos(r'+s')H+3451535\cos(r'-s')H, \quad (31)$$

$$\Delta_C=336645+2086088\cos(r'+s')H+574416\cos(r'-s')H$$
$$-i2086088\sin(r'+s')H-i574416\sin(r'-s')H, \quad (32)$$

$$\Delta_D=413626-622049\cos(r'+s')H-1926347\cos(r'-s')H$$
$$-i622049\sin(r'+s')H-i1926347\sin(r'-s')H, \quad (33)$$

$$\Delta_E=179836-811769\cos(r'+s')H-610075\cos(r'-s')H$$
$$+i811769\sin(r'+s')H-i610075\sin(r'-s')H, \quad (34)$$

$$\Delta_F=603094+660665\cos(r'+s')H+749609\cos(r'-s')H$$
$$+i660665\sin(r'+s')H-i749609\sin(r'-s')H, \quad (35)$$

11) K. Sezawa has already studied the orbital motion of the top surface particle in the surface layer when $\rho=\rho'$, $\lambda=\lambda'$, $\mu=\mu'$, $\theta=45°$ and $\mu'/\mu=1/2$. K. SEZAWA and K. KANAI, *Bull. Earthq. Res. Inst.*, **10** (1932), 806; **12** (1934), 269.

where

$$r'H = 19{\cdot}3657\left(\frac{H}{L}\right), \qquad sH = 34{\cdot}1264\left(\frac{H}{L}\right). \tag{36}$$

The values A, B, C, D, E, and F, therefore, become complex values which are transcendental functions, only H/L being variable.

We have calculated the values of A, B, C, D, E, and F for various values of H/L as shown in Table I.

Table I.

$\frac{H}{L}$	A	B	C	D	E	F
0·01	−0·2900 +i0·01738	0·6263 +i0·1311	0·2524 −i0·03596	−0·1755 −i0·03980	−0·1066 +i0·02334	0·1581 +i0·07362
0·02	−0·3203 +i0·04315	0·5704 +i0·2743	0·2631 −i0·07389	−0·1699 −i0·07989	−0·1196 +i0·04972	0·1228 +i0·1552
0·03	−0·457 +i0·07623	0·4270 +i0·4301	0·2871 −i0·1142	−0·1645 −i0·1210	−0·1551 +i0·07910	0·02932 +i0·2448
0·04	−0·6803 −i0·003673	0·09698 +i0·4805	0·3333 −i0·1454	−0·1745 −i0·1795	−0·2426 +i0·07678	−0·1935 +i0·2585
0·048	−0·8279 −i0·4387	−0·1176 +i0·2021	0·3682 −i0.1489	−0·1689 −i0·2937	−0·2964 −i0·02473	−0·3342 +i0·03464
0·05	−0·7827 −i0·5753	−0·1043 +i0·1188	0·3733 −i0·1513	−0·1512 −i0·3311	−0·2884 −i0·05594	−0·3194 −i0·03344
0·06	−0·2547 −i0·9607	0·07335 −i0·001686	0·4259 −i0·1925	0·04661 −i0·4789	−0·1910 −i0·1256	−0·1341 −i0·1638
0·07	0·4040 −i0·9141	0·01668 +i0·01349	0·5753 −i0·1877	0·3963 −i0·4612	−0·1141 −i0·1171	−0·0530 −i0·1477
0·08	0·8919 −i0·02904	−0·02670 −i0·2301	0·6863 +i0·01089	0·6559 −i0·05989	−0·05745 −i0·07488	0·006337 −i0·1733
0·09	0·6612 +i0·3374	0·2404 −i0·3772	0·5596 +i0·1813	0·4420 +i0·3079	−0·04461 −i0·01663	0·1112 −i0·1462
0·10	0·3057 +i0·5152	0·4620 −i0·2706	0·4215 +i0·1850	0·1826 +i0·3572	−0·05534 +i0·02369	0·1705 −i0·05858
0·11	0·1014 +i0·5494	0·5458 −i0·09830	0·3545 +i0·1403	0·04778 +i0·3111	−0·06902 +i0·05588	0·1804 +i0·03998
0·12	−0·04678 +i0·6060	0·5243 +i0·08470	0·3319 +i0·09623	−0·01636 +i0·2711	−0·09132 +i0·09267	0·1443 +i0·1484
0·13	−0·2665 +i0·7236	0·3488 +i0·2442	0·3406 +i0·07184	−0·06111 −i0·2708	−0·1482 +i0·13337	0·01243 +i0·2543
0·14	−0·7474 +i0·6470	0·02267 +i0·09876	0·3422 +i0·1002	−0·1805 +i0·2864	−0·2634 +i0·1003	−0·2449 +i0·1629
0·146	−0·9121 +i0·3243	0·04810 −i0·1609	0·3014 +i0·1136	−0·2721 +i0·2213	−0·2808 +i0·01645	−0·2591 −i0·03174
0·15	−0·8805 +i0·1346	0·1503 −i0·2425	0·2770 +i0·1000	−0·2942 +i0·1569	−0·2602 −i0·02140	−0·1987 −i0·1079

(to be continued.)

Table I. (*continued*)

$\frac{H}{L}$	*A*	*B*	*C*	*D*	*E*	*F*
0·16	−0·6951 −*i*0·1003	0·4194 −*i*0·2253	0·2333 +*i*0·04766	−0·3012 +*i*0·03325	−0·1927 −*i*0·04930	−0·02214 −*i*0·1384
0·17	−0·5831 −*i*0·1681	0·5227 −*i*0·09612	0·2246 −*i*0·004865	−0·2835 −*i*0·04843	−0·1615 −*i*0·03740	0·05252 −*i*0·08033
0·18	−0·5350 −*i*0·2163	0·5449 +*i*0·03658	0·2276 −*i*0·05445	−0·2677 −*i*0·1215	−0·1517 −*i*0·02233	0·07266 −*i*0·01694
0·19	−0·5274 −*i*0·2876	0·5101 +*i*0·1674	0·2407 −*i*0·1082	−0·2485 −*i*0·2055	−0·1557 −*i*0·01061	0·05598 +*i*0·04148
0·20	−0·5221 −*i*0·4262	0·3998 +*i*0·2903	0·2739 −*i*0·1730	−0·2076 −*i*0·3201	−0·1733 −*i*0·00893	−0·003397 +*i*0·08425
0·21	−0·4378 −*i*0·7121	0·1650 +*i*0·3278	0·3615 −*i*0·2417	−0·07867 −*i*0·4766	−0·2001 −*i*0·04021	−0·1157 +0·05599
0·22	0·07050 −*i*0·9944	−0·01654 +*i*0·05123	0·5182 −*i*0·2151	0·2422 −*i*0·5153	−0·1629 −*i*0·1215	−0·1274 −*i*0·1409
0·23	0·6484 −*i*0·6635	0·2296 −*i*0.09769	0·5603 −*i*0·1039	0·4396 −*i*0·2950	−0·04799 −*i*0·1023	0·1033 −*i*0·01651
0·24	0·8830 −*i*0·1794	0·2767 +*i*0·08641	0·5932 −*i*0·06207	0·5393 −*i*0·1215	−0·009823 −*i*0·009514	0 1684 +*i*0·01617
0·25	0·8653 +*i*0·4845	0·04180 +*i*0·07509	0·6603 +*i*0·07471	0·6173 +*i*0·2140	−0·04990 +0·07528	0·03877 +*i*0·1226
0·26	0·2670 +*i*0·8976	0·6557 −*i*0·2258	0·5331 +*i*0·2482	0·3099 +*i*0·5315	−0·1241 +*i*0 08080	−0·04985 +*i*0·03045
0·27	−0·1903 +*i*0·7610	0·3093 −*i*0·2763	0·3678 +*i*0·2360	−0·00847 +*i*0·4820	−0·1446 +*i*0·05485	0·00403 −*i*0·01997
0·28	−0·3754 +*i*0·5888	0·4486 −*i*0·1672	0·2887 +*i*0·1686	−0·1524 +*i*0·3557	−0·1464 +*i*0·04993	0·04777 +*i*0·009689
0·29	−0·4848 +*i*0·4843	0·4864 −*i*0·02598	0·2554 +*i*0·1053	−0·2210 +*i*0·2513	−0·1546 +*i*0·0590	0·04958 +*i*0·06809
0·30	−0·6200 +*i*0·4142	0·4294 +*i*0·1191	0·2453 +*i*0·04930	−0·2674 +*i*0·1627	−0·1814 +*i*0·07318	−0·004081 +*i*0·1344
0·31	−0·8554 +*i*0·2662	0·2201 +*i*0·1997	0·2611 −*i*0·00664	−0·3075 +*i*0·05902	−0·2457 +*i*0·06682	−0·1568 +*i*0·1528
0·32	−0·9637 −*i*0·2337	−0·00547 −*i*0·08623	0·3072 −*i*0·02099	−0·2781 −*i*0·08476	−0·2961 −*i*0·04435	−0·2968 −*i*0·08612
0·33	−0·5461 −*i*0·5079	0·2907 −*i*0·3375	0·3019 −*i*0·00043	−0·1792 −*i*0·1287	−0·1940 −*i*0·1206	−0·06628 −*i*0·2681
0·34	−0·3070 −*i*0·4319	0·5226 −*i*0·2214	0·2805 −*i*0·02013	−0·1448 −*i*0·1337	−0·1253 −*i*0·09193	0·09951 −*i*0·1926
0·35	−0·2129 −*i*0·3700	0·6014 −*i*0·06320	0·2753 −*i*0·05531	−0·1278 −*i*0·1613	−0·1006 −*i*0·05843	0·1577 −*i*0·09680

(*to be continued.*)

Table I. (*continued.*)

$\frac{H}{L}$	A	B	C	D	E	F
0·36	−0·1532 −i0·3509	0·6117 +i0·08624	0·2842 −i0·09645	−0·1018 −i0·2065	−0·09114 −i0·03191	0·1734 −i0·01299
0·37	−0·08177 −i0·3605	0·5749 +i0·2359	0·3097 −i0·1434	−0·05252 −i0·2672	−0·08775 −i0·00910	0·1656 +i0·06609
0·38	0·03885 −i0·3800	0·4746 +i0·3959	0·3641 −i0·1955	0·04477 −i0·3361	−0·08814 +i0·01407	0·1320 +i0·1490
0·39	0·2626 −i0·3438	0·2515 +i0·5480	0·4762 −i0·2340	0·2389 −i0·3742	−0·09481 +i0·04326	0·04968 +i0·2372
0·40	0·5351 −i0·01646	−0·1723 +i0·5382	0·6585 −i0·1653	0·5317 −i0·2072	−0·1274 +i0·08438	−0·1327 +i0·2874
0·41	0·2302 +i0.5118	−0·5512 +i0·05002	0·7112 +i0·08777	0·5195 +i0·2370	−0·2281 +i0·01481	−0·3887 +i0·1137
0·42	−0·1461 +i0·3267	−0·2375 −i0·5773	0·5413 +i0·2394	0·2158 +i0·3765	−0·2268 −i0·05021	−0·2833 −i0·2559
0·43	−0·1493 +i0·2308	0·2554 −i0·5901	0·3923 +i0·2240	0·03189 +i0·3334	−0·1479 −i0·06478	−0·01803 −i0·2791
0·44	−0·1734 +i0·2169	0·4856 −i0·4207	0·3181 +i0·1702	−0·06523 +i0·2639	−0·1141 −i0·03934	0·1019 −i0·1900
0·45	−0·2026 +i0·2074	0·5850 −i0·2597	0·2824 +i0·1198	−0·1166 +i0·1996	−0·1019 −i0·01469	0·1506 −i0·1048
0·46	−0·2281 +i0·2045	0·6257 −i0·1172	0·2650 +i0·07635	−0·1444 +i0·1454	−0·09866 +i0·007830	0·1682 −i0·02853
0·47	−0·2550 +i0·2150	0·6302 +i0·01860	0·2582 +i0·03760	−0·1595 +i0·1002	−0·1015 +i0·03104	0·1661 +i0·04647
0·48	−0·2982 +i0·2181	0·5951 +i0·1601	0·2601 +i0·001499	−0·1680 +i0·06445	−0·1127 +i0·05819	0·1398 +i0·1286
0·49	−0·4013 +i0·3112	0·4835 +i0·3133	0·2730 −i0·03177	−0·1782 +i0·03949	−0·1441 +i0·09097	0·06220 +i0·2217
0·50	−0·6874 +i0·3272	0·1999 +i0·3848	0·3008 −i0·05010	−0·2161 +i0·02101	−0·2270 +i0·1046	−0·1392 +i0·2629
0·51	−0·9911 −i0·1167	−0·01575 +i0·04249	0·3048 −i0·03623	−0·2880 −i0·07397	−0·3013 −i0·00839	−0·3069 +i0·003146
0·52	−0·7262 −i0·5399	0·2513 −i0·1332	0·2776 −i0·06838	−0·2546 −i0·2202	−0·2239 −i0·09184	−0·1181 −i0·1633
0·53	−0·4597 −i0·6680	0·3912 −i0·00976	0·2890 −i0·1313	−0·1732 −i0·3298	−0·1666 −i0·08871	0·00253 −i0·1185
0·54	−0·2259 −i0·7822	0·3628 +i0·1383	0·3446 −i0·1988	−0·04603 −i0·4416	−0·1406 −i0·07982	0·02685 −i0·05806
0·55	0·1573 −i0·8913	0·1920 +i0·2099	0·4729 −i0·2422	0·2084 −i0·5225	−0·1181 −i0·08254	−0·00028 −i0·03795

(*to be continued.*)

Table I. (*continued.*)

$\frac{H}{L}$	A	B	C	D	E	F
0·56	0·8097 $-i$0·5435	$-$0·000271 $-i$0·02810	0·6619 $-i$0·1007	0·6051 $-i$0·2609	$-$0·06393 $-i$0·07543	0·00665 $-i$0·1073
0·57	0·9062 $+i$0·08601	0·1720 $-i$0·2176	0·6294 $+i$0·08278	0·5896 $+i$0·1234	$-$0·02364 $-i$0·02377	0·1159 $-i$0·1027
0·58	0·6069 $+i$0·5071	0·3899 $-i$0·1238	0·5037 $+i$0·1392	0·3596 $+i$0·2989	$-$0·02765 $+i$0·04625	0·1826 $+i$0·01920
0·59	0·3322 $+i$0·7449	0·3768 $+i$0·08694	0·4524 $+i$0·1235	0·2273 $+i$0·3397	$-$0·06557 $+i$0·1112	0·1290 $+i$0·1732
0·60	$-$0·1102 $+i$0·9639	0·09750 $+i$0·1301	0·4476 $+i$0·1544	0·1098 $+i$0·4330	$-$0·1682 $+i$0·1467	$-$0·09655 $+i$0·2335
0·62	$-$0·6685 $+i$0·2862	0·3361 $-i$0·3129	0·2637 $+i$0·1517	$-$0·2571 $+i$0·2586	$-$0·2027 $-i$0·01298	$-$0·06259 $-i$0·1202
0·885	0·3189 $-i$0·8110	$-$0·3082 $-i$0·1115	0·6559 $-i$0·1294	$-$0·4740 $-i$0·3636	$-$0·1775 $-i$0·1237	$-$0·2426 $-i$0·1976
1·205	0·5145 $-i$0·3859	0·2771 $+i$0·4306	0·5191 $-i$0·2071	0·3552 $-i$0·3519	$-$0·05784 $+i$0·01889	0·1062 $+i$0·1668
1·525	0·5316 $-i$0·6787	0·3314 $-i$0·06654	0·5061 $-i$0·1163	0·3436 $-i$0·3141	$-$0·04688 $-i$0·09924	0·1383 $-i$0·1509
1·845	0·03301 $-i$0·8618	0·2226 $+i$0·25503	0·4387 $-i$0·2499	0·1350 $-i$0·5245	$-$0·1294 $-i$0·07142	$-$0·00484 $-i$0·00860
2·165	$-$0·6765 $-i$0·5605	$-$0·1947 $+i$0·2536	0·4218 $-i$0·1889	$-$0·06479 $-i$0·3735	$-$0·2891 $-i$0·03234	$-$0·3501 $+i$0·04173
2·485	0·01920 $-i$0·4298	0·5465 $+i$0·2565	0·3385 $-i$0·1635	0·00835 $-i$0·3094	$-$0·07914 $-i$0·01483	0·1674 $+i$0·06543
2·805	$-$0·2088 $-i$0·9627	0·05807 $-i$0·09933	0·4397 $-i$0·1635	0·07520 $-i$0·4438	$-$0·1874 $-i$0·1416	$-$0·1345 $-i$0·2168

2. *The Orbital motion of a Surface Particle in the Surface Layer.*

Now, taking the real parts only, we get the following horizontal and vertical oscillations U' and V' on the top surface of the surface layer.

$$\left.\frac{LU'}{2\pi a}\right]_{x=0}=\cos\theta\cos z\Big[(C'-D')\sin a-(C''+D'')\cos a$$

$$+\frac{s'}{f}\Big\{-(E'+F')\sin b+(E''-F'')\cos b\Big\}\Big]$$

$$+\cos\theta\sin z\Big[(C'-D'')\sin b+(C'+D')\cos a$$

$$+\frac{s'}{f}\Big\{-(E''+F')\sin b+(-E'+F')\cos b\Big], \qquad (37)$$

$$\left.\frac{LV'}{2\pi a}\right]_{x=0}=\cos\theta\cos z\left[\frac{r'}{f}\left\{-(C'+D')\sin a+(C''-D'')\cos a\right\}\right.$$
$$\left.-(E'-F')\sin b+(E''+F'')\cos b\right]$$
$$+\cos\theta\sin z\left[\frac{r'}{f}\left\{-(C''+D'')\sin a+(-C'+D')\cos a\right\}\right.$$
$$\left.-(E''-F'')\sin b-(E'+F')\cos b\right], \qquad (38)$$

where $z=\frac{2\pi}{T}t$, $\frac{r'}{f}=4{\cdot}3588$, $\frac{s'}{f}=7{\cdot}6811$, $a=19{\cdot}3657\left(\frac{H}{L}\right)$ and $b=34{\cdot}1264\left(\frac{H}{L}\right)$. As will be seen from the following expressions (39), C', D', E', and F' are real parts of C, D, E, and F respectively, while C'', D'', E'', and F'' correspond to imaginary parts of them:

$$\left.\begin{aligned} C&=C'+iC'', & D&=D'+iD'', \\ E&=E'+iE'', & F&=F'+iF''. \end{aligned}\right\} \qquad (39)$$

Expressions (37), (38) are next rewritten:

$$\left.\frac{LU'}{2\pi a}\right]_{x=0}=\sqrt{\alpha^2+\beta^2}\sin\left\{z+\tan^{-1}\frac{\beta}{\alpha}\right\}, \qquad (40)$$

$$\left.\frac{LV'}{2\pi a}\right]_{x=0}=\sqrt{\alpha'^2+\beta'^2}\sin\left\{z+\tan^{-1}\frac{\beta'}{\alpha'}\right\}, \qquad (41)$$

where

$$\alpha=\left\{(C''-D'')\sin b+(C'+D')\cos a\right\}$$
$$+\frac{s'}{f}\left\{-(E''+F'')\sin b+(-E'+F')\cos b\right\}, \qquad (42)$$

$$\beta=\left\{(C'-D')\sin a-(C''+D'')\cos a\right\}$$
$$+\frac{s'}{f}\left\{-(E'+F')\sin b+(E''-F'')\cos b\right\}, \qquad (43)$$

$$\alpha'=\frac{r'}{f}\left\{-(C''+D'')\sin a+(-C'+D')\cos a\right\}$$
$$+\left\{-(E''-F'')\sin b-(E'+F')\cos b\right\}, \qquad (44)$$

$$\beta'=\frac{\gamma'}{f}\left\{-(C'+D')\sin a+(C''-D'')\cos a\right\}$$

$$+\left\{-(E'-F')\sin b+(E''+F'')\cos b\right\}, \tag{45}$$

and the values α, β, α', β' become circular functions, $H\,L$ alone being variable. $\tan^{-1}(\beta\,\alpha)$ and $\tan^{-1}(\beta'/\alpha')$ should be taken satisfying the conditions that

$$\left.\begin{aligned}\sqrt{\alpha^2+\beta^2}\sin\gamma&=\alpha,\\ \sqrt{\alpha^2+\beta^2}\cos\gamma&=\beta,\\ \gamma&=\tan^{-1}\frac{\beta}{\alpha},\end{aligned}\right\}$$

$$\left.\begin{aligned}\sqrt{\alpha'^2+\beta'^2}\sin\gamma'&=\alpha',\\ \sqrt{\alpha'^2+\beta'^2}\cos\gamma'&=\beta',\\ \gamma'&=\tan^{-1}\frac{\beta'}{\alpha'}.\end{aligned}\right\}$$

It will be seen from expressions (40), (41) that forced stationary harmonic vibrations (horizontal and vertical) are caused in the stratum by the periodic incident wave (1). The amplitudes of the same vibrations (vertical and horizontal) and the phase-differences are both transcendental functions, only H/L being variable. The phases of the vibrations on the free surface of the layer usually differ from those of vibrations (horizontal and vertical respectively) at the bottom surface. We shall return to the horizontal and vertical stationary oscillations (40) and (41) in the next chapter.

Now we can easily get from expressions (40) and (41) the orbit of the particle in the surface layer as follows:

$$\frac{U'^2}{(\alpha^2+\beta^2)}+\frac{V'^2}{(\alpha'+\beta'^2)}-\frac{2\cos\varepsilon}{\sqrt{\alpha^2+\beta^2}\sqrt{\alpha'^2+\beta'^2}}U'V'=\frac{4\pi^2\mathfrak{a}^2}{L^2}\sin^2\varepsilon, \tag{46}$$

where

$$\varepsilon=\tan^{-1}\frac{\beta'}{\alpha'}-\tan^{-1}\frac{\beta}{\alpha}. \tag{47}$$

It will be seen from expression (46) that the orbit of the particle in the surface layer is usually an ellipse, whose major and minor axes ξ, η are respectively given by

$$\left.\begin{aligned} \xi &= \frac{\sin\varepsilon}{\sqrt{\gamma}}, \\ \eta &= \frac{\sin\varepsilon}{\sqrt{\delta}}, \end{aligned}\right\} \tag{48}$$

where γ, δ are the roots of the equation

$$\zeta^2 - \frac{(\alpha^2+\beta^2+\alpha'^2+\beta'^2)}{(\alpha^2+\beta^2)(\alpha'^2+\beta'^2)}\zeta + \frac{\sin^2\varepsilon}{(\alpha^2+\beta^2)(\alpha'^2+\beta'^2)} = 0, \tag{48'}$$

the inclination angle τ which the major axis makes with the horizontal surface being

$$\tan 2\tau = -\frac{2\cos\varepsilon\sqrt{(\alpha^2+\beta^2)(\alpha'^2+\beta'^2)}}{(\alpha'^2+\beta'^2)-(\alpha^2+\beta^2)}. \tag{49}$$

We calculated the major and minor axes of the elliptic orbit of the particles on the top and the bottom surfaces of the surface layer, the ratio of the minor to the major axes, and the inclination angle of the same elliptic orbit for several cases of H/L, the results being given in Table II and Table III, and shown in Figs. 2～7.

Table II. Major and Minor Axes of Elliptic Orbit of Particle on Top Surface.

$\frac{H}{L}$	ξ (Major axis)	η (Minor axis)	η/ξ	τ (Inclination of major axis in degrees)
0·01	2·08	0·10	0·048	41°
0·02	2·32	0·20	0·086	38°
0·03	2·80	0·45	0·160	35°
0·04	3·55	1·12	0·316	28°
0·05	3·90	2·25	0·577	35°
0·06	3·00	2·30	0·767	99°
0·07	3·85	1·46	0·376	90°
0·08	4·54	1·05	0·231	86°
0·09	3·73	0·50	0·134	73°
0·10	2·95	0·40	0·135	66°
0·11	2·60	0·46	0·203	57°
0·12	2·50	0·75	0·30	46°
0·13	2·85	1·36	0·477	34°
0·14	3·10	2·14	0·691	10°
0·15	2·85	1·70	0·596	154°

(*to be continued.*)

Table II. (*continued.*)

$\frac{H}{L}$	ξ (Major axis)	η (Minor axis)	η/ξ	τ (Inclination of major axis)
0·16	2·46	1·03	0·429	136°
0·17	2·15	0·44	0·205	130°
0·18	2·08	0·14	0·0673	128°
0·19	2·17	0·20	0·0922	125°
0·20	2·57	0·64	0·249	121°
0·21	3·22	1·30	0·4035	113°
0·22	3·55	1·94	0·546	98°
0·23	3·88	1·25	0·322	76°
0·24	3·75	0·14	0·0373	76°
0·25	4·17	0·55	0·1318	92°
0·26	3·84	0·50	0·132	99°
0·27	3·05	0·145	0·0492	108°
0·28	2·54	0·15	0·0590	116°
0·29	2·34	0·50	0·214	125°
0·30	2·40	0·900	0·375	137°
0·31	2·78	1·50	0·540	157°
0·32	3·40	1·77	0 521	5°
0·33	3·03	1·20	0·364	25°
0·34	2·84	0·65	0·230	44°
0·35	2·24	0·40	0·1785	43°
0·36	2·20	0·34	0·154	50°
0·37	2·43	0·25	0·1028	53°
0·38	2·90	0 30	0·1034	57°
0·39	3·59	0·54	0·1504	58°
0·40	4·55	1·02	0·224	58°
0·41	5·45	0	0	49°
0·42	4·70	0·50	0·1063	44°
0·43	3·50	0·10	0·0286	46°
0·44	2·68	0·07	0·0161	47°
0·45	2·34	0·10	0·0428	47°
0·46	2·10	0·15	0·0714	45°
0·47	2·05	0·20	0·098	45°
0·48	2·20	0·32	0·1454	38°
0·49	2·63	0·61	0·232	31°
0·50	3·23	1·18	0·365	21°
0·51	3·35	1·89	0·564	179°
0·52	2·67	1·60	0·60	150°
0·53	2·57	1·04	0·405	125°
0·54	2·85	0·64	0·2245	111°
0·55	3·51	0·31	0·088	102°
0·56	4·20	0·28	0·0667	90°
0·57	3·95	0·65	0·1645	86°
0·58	3·30	0·45	0·1363	68°
0·59	3·14	1·25	0·398	60°
0·60	3·10	2·37	0·764	55°

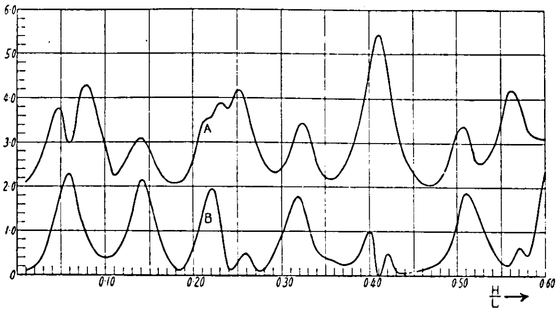

Fig. 2. Major and minor axes of the elliptic orbits of a particle on the top surface of the surface layer. A: Major axis, B: Minor axis.

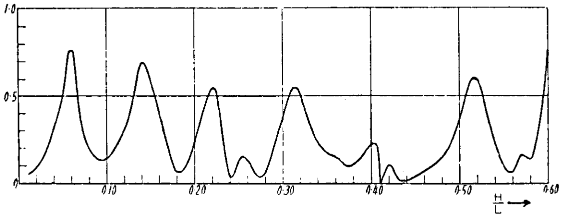

Fig. 3. Ratio of the minor to the major axes of the elliptic orbits of the particle on the top surface of the surface layer.

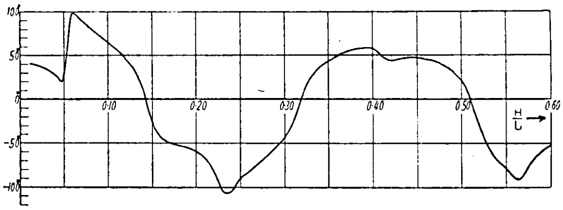

Fig. 4. Inclination angle of the elliptic orbit of the particle on the top surface of the surface layer.

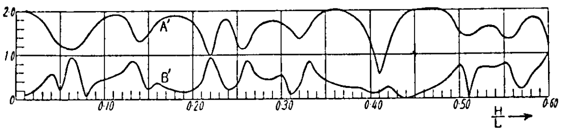

Fig. 5. Major and minor axes of the elliptic orbit of the particle on the bottom surface of the surface layer. A′: Major axis, B′: Minor axis.

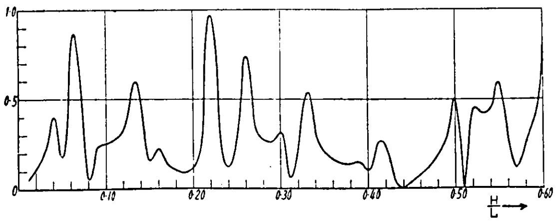

Fig. 6. Ratio of the minor to the major axes of the elliptic orbits of the particles on the bottom surface of the surface layer.

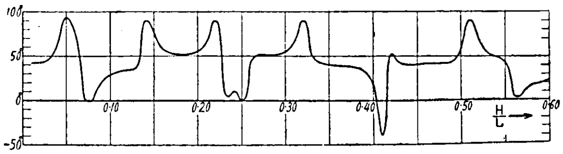

Fig. 7. Inclination angle of the elliptic orbit of the particle on the bottom surface of the surface layer.

Table III. Major and Minor Axes of Elliptic Orbit of Particle on Bottom Surface.

$\frac{H}{L}$	ξ' (Major axis)	η' (Minor axis)	η'/ξ'	τ' (Inclination of major axis)
0·01	2·03	0·10	0·0493	42°
0·02	1·95	0·20	0·1025	43°
0·03	1·79	0·36	0·201	45°
0·04	1·45	0·58	0·400	62°
0·05	1·25	0·22	0·176	94°
0·06	1·16	0·90	0·776	77°
0·07	1·18	0·80	0·678	2°
0·08	1·43	0·08	0·056	1°
0·09	1·67	0·38	0·2275	20°
0·10	1·85	0·46	0·2485	29°
0·11	1·92	0·52	0·271	32°
0·12	1·90	0·61	0·321	34°
0·13	1·61	0·87	0·540	36°
0·14	1·31	0·65	0·496	89°·5
0·15	1·50	0·23	0·1533	75°
0·16	1·75	0·38	0·217	57°
0·17	1·85	0·25	0·135	54°
0·18	1·90	0·20	0·1052	52°
0·19	1·85	0·15	0·0811	52°
0·20	1·75	0·20	0·1143	55°

(*to be continued.*)

Table III. (*continued.*)

$\frac{H}{L}$	ξ' (Major axis)	η' (Minor axis)	$\eta' : \xi'$	τ' (Inclination of major axis)
0·21	1·45	0·36	0·2481	66°
0·22	0·99	0·97	0·970	90°
0·23	1·68	0·52	0·3095	8°
0·24	1·79	0·21	0·1173	9°
0·25	1·25	0·32	0·256	0°
0·26	1·18	0·87	0·737	43°
0·27	1·58	0·57	0·361	52°
0·28	1·72	0·47	0·273	51°
0·29	1·76	0·45	0·256	52°
0·30	1·71	0·53	0·310	55°
0·31	1·60	0·10	0·0625	65°
0·32	1·36	0·30	0·2205	90°·5
0·33	1·57	0·83	0·529	51°
0·34	1·85	0·58	0·3135	41°·5
0·35	1·95	0·41	0·210	40°
0·36	2·00	0·33	0·165	39°
0·37	1·98	0·27	0·1363	38°
0·38	1·86	0·25	0·1344	37°
0·39	1·70	0·24	0·1412	33°
0·40	1·25	0·125		21°
0·41	0·55	0·13	0·2363	141°
0·42	1·15	0·27	0·2347	52°
0·43	1·70	0·110	0·0588	42°
0·44	1·93	0	0	41°
0·45	2·00	0·08	0·040	41°
0·46	2·04	0·15	0·0736	40°·5
0·47	2·04	0·23	0·1128	41°
0·48	2·00	0·35	0·175	42°
0·49	1·85	0 51	0·276	43°
0·50	1·50	0·75	0·500	59°
0·51	1·40	0	0	90°
0·52	1·50	0·66	0·440	69°
0·53	1·62	0 68	0·4195	53°
0·54	1·60	0·70	0·438	49°
0·55	1·35	0·80	0·593	42°
0·56	1·35	0·40	0·2963	4°
0·57	1·63	0·18	0·1105	8°
0·58	1·82	0·48	0·2637	18°
0·59	1·78	0·69	0·388	19°
0·60	1·23	1·00	0·8130	23°

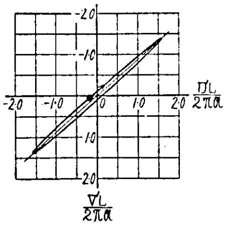

Fig. 8. $\frac{H}{L}=0{\cdot}01$, x=0, y=−H.

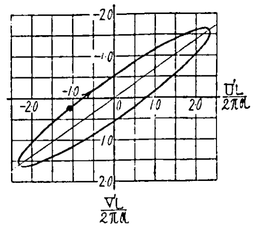

Fig. 12. $\frac{H}{L}=0{\cdot}03$, x=0, y=−H.

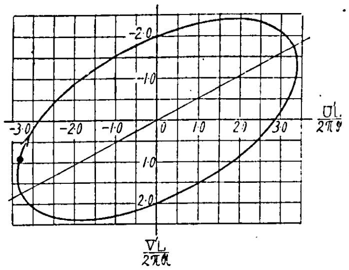

Fig. 16. $\frac{H}{L}=0{\cdot}05$, x=0, y=−H.

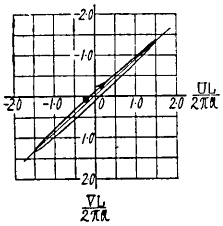

Fig. 9. $\frac{H}{L}=0{\cdot}01$, x=0, y=0.

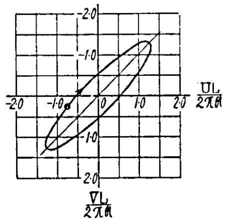

Fig. 13. $\frac{H}{L}=0{\cdot}03$, x=0, y=0.

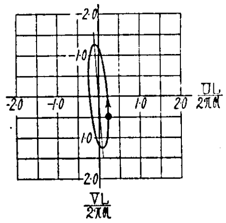

Fig. 17. $\frac{H}{L}=0{\cdot}05$, x=0, y=0.

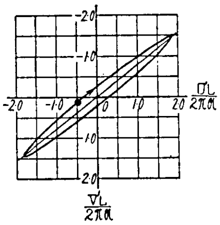

Fig. 10 $\frac{H}{L}=0{\cdot}02$, x=0, y=−H.

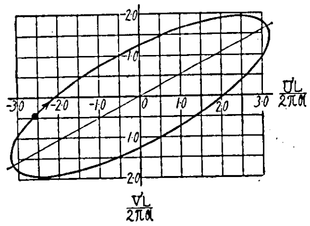

Fig. 14. $\frac{H}{L}=0{\cdot}04$, x=0, y=−H.

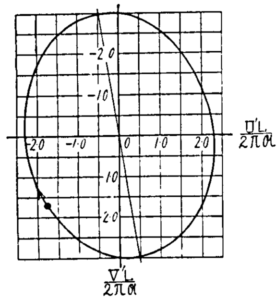

Fig. 18. $\frac{H}{L}=0{\cdot}06$, x=0, y=−H.

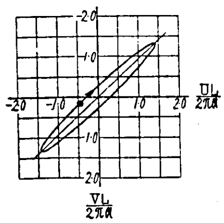

Fig. 11. $\frac{H}{L}=0{\cdot}02$, x=0, y=0.

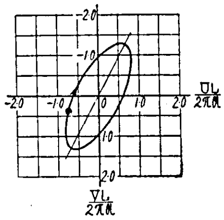

Fig. 15. $\frac{H}{L}=0{\cdot}04$, x=0, y=0.

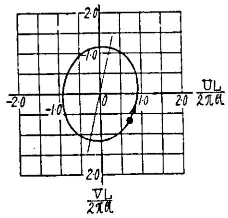

Fig. 19. $\frac{H}{L}=0{\cdot}06$, x=0, y=0.

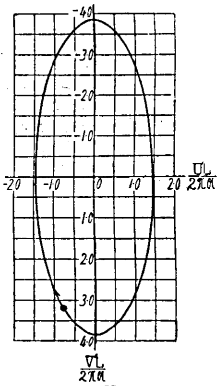

Fig. 20. $\frac{H}{L}=0{\cdot}07$, $x=0$, $y=-H$.

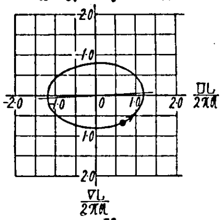

Fig. 21. $\frac{H}{L}=0{\cdot}07$, $x=0$, $y=0$.

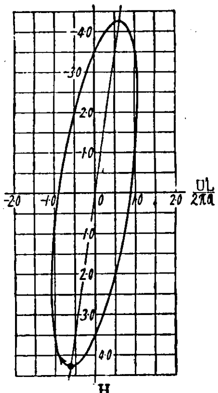

Fig. 22. $\frac{H}{L}=0{\cdot}08$, $x=0$, $y=-H$.

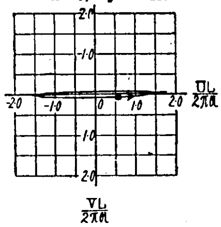

Fig. 23. $\frac{H}{L}=0{\cdot}08$, $x=0$, $y=0$.

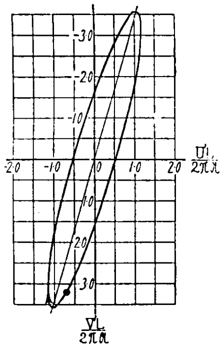

Fig. 24. $\frac{H}{L}=0{\cdot}09$, $x=0$, $y=-H$.

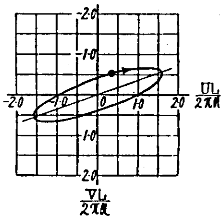

Fig. 25. $\frac{H}{L}=0{\cdot}09$, $x=0$, $y=0$.

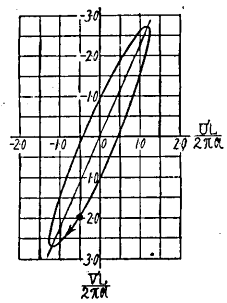

Fig. 26. $\frac{H}{L}=0{\cdot}10$, $x=0$, $y=-H$.

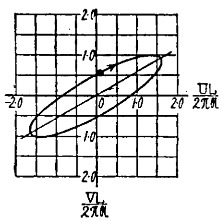

Fig. 27. $\frac{H}{L}=0{\cdot}10$, $x=0$, $y=0$.

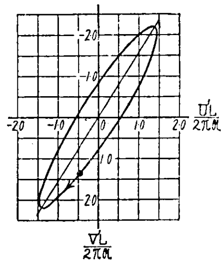

Fig. 28. $\frac{H}{L}=0{\cdot}11$, $x=0$, $y=-H$.

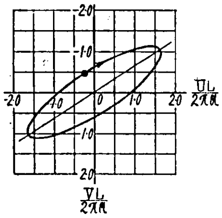

Fig. 29. $\frac{H}{L}=0{\cdot}11$, $x=0$, $y=0$.

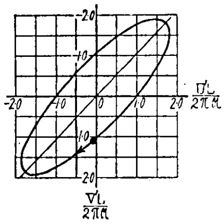

Fig. 30. $\frac{H}{L}=0{\cdot}12$, $x=0$, $y=-H$.

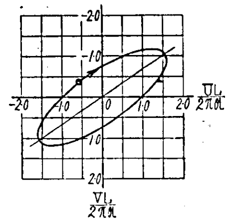

Fig. 31. $\frac{H}{L}=0{\cdot}12$, $x=0$, $y=0$.

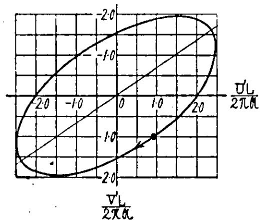

Fig. 32. $\frac{H}{L}=0{\cdot}13$,
x = 0, y = −H.

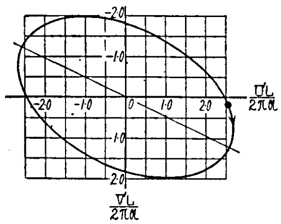

Fig. 36. $\frac{H}{L}=0{\cdot}15$,
x = 0, y = −H.

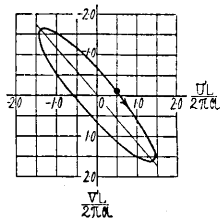

Fig. 40. $\frac{H}{L}=0{\cdot}17$,
x = 0, y = −H.

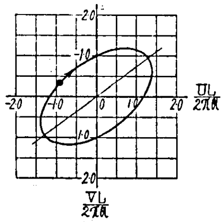

Fig. 33. $\frac{H}{L}=0{\cdot}13$,
x = 0, y = 0.

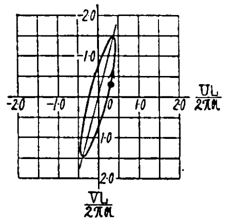

Fig. 37. $\frac{H}{L}=0{\cdot}15$,
x = 0, y = 0.

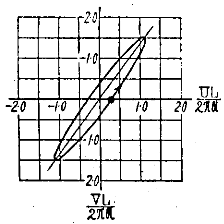

Fig. 41. $\frac{H}{L}=0{\cdot}17$,
x = 0, y = 0.

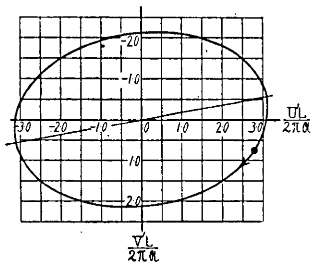

Fig. 34. $\frac{H}{L}=0{\cdot}14$,
x = 0, y = −H.

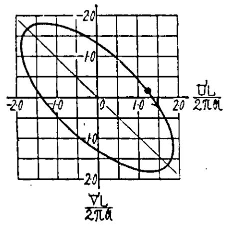

Fig. 38. $\frac{H}{L}=0{\cdot}16$,
x = 0, y = −H.

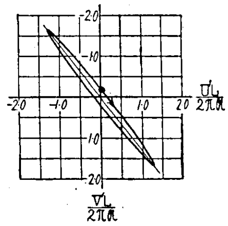

Fig. 42. $\frac{H}{L}=0{\cdot}18$,
x = 0, y = −H.

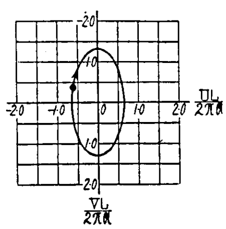

Fig. 35. $\frac{H}{L}=0{\cdot}14$,
x = 0, y = 0.

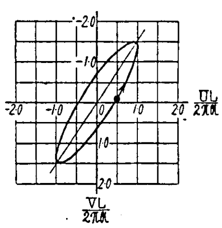

Fig. 39. $\frac{H}{L}=0{\cdot}16$,
x = 0, y = 0.

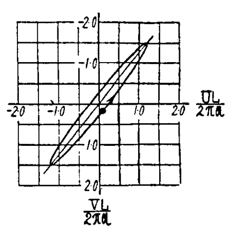

Fig. 43. $\frac{H}{L}=0{\cdot}18$,
x = 0, y = 0.

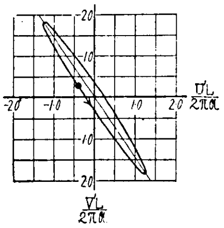

Fig. 44. $\frac{H}{L}=0{\cdot}19$,

x=0, y=−H.

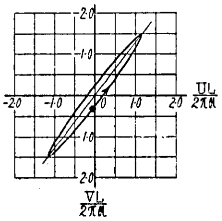

Fig. 45. $\frac{H}{L}=0{\cdot}19$,

x=0, y=0.

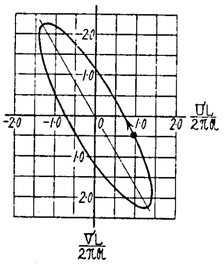

Fig. 46. $\frac{H}{L}=0{\cdot}20$,

x=0, y=−H.

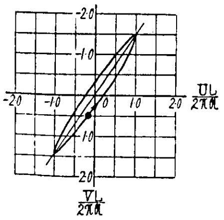

Fig. 47. $\frac{H}{L}=0{\cdot}20$,

x=0, y=0.

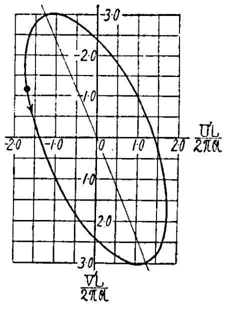

Fig. 48. $\frac{H}{L}=0{\cdot}21$,

x=0, y=−H.

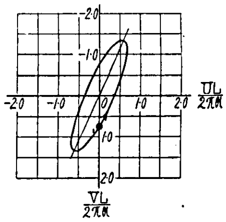

Fig. 49. $\frac{H}{L}=0{\cdot}21$,

x=0, y=0.

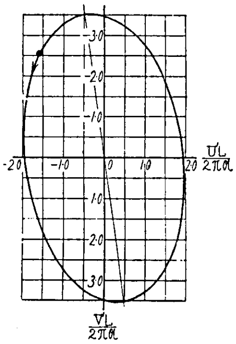

Fig. 50. $\frac{H}{L}=0{\cdot}22$,

x=0, y=−H.

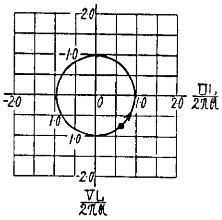

Fig. 51. $\frac{H}{L}=0{\cdot}22$,

x=0, y=0.

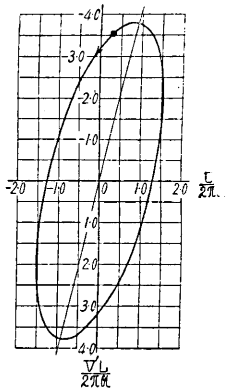

Fig. 52. $\frac{H}{L}=0{\cdot}23$,

x=0, y=−H.

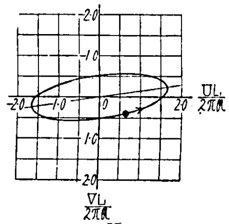

Fig. 53. $\frac{H}{L}$ 0.23,

x=0, y=0.

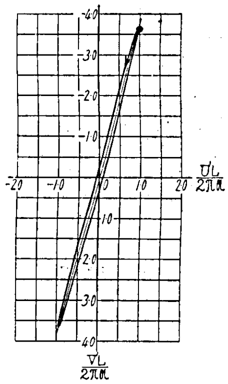

Fig. 54. $\frac{H}{L}=0{\cdot}24$,

x=0, y=−H.

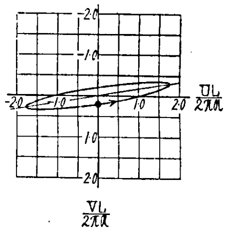

Fig. 55. $\frac{H}{L}=0{\cdot}24$,

x=0. y=0.

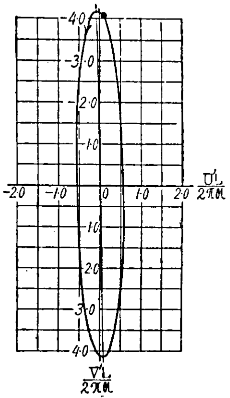

Fig. 56. $\frac{H}{L}=0{\cdot}25$,

x=0, y=−H.

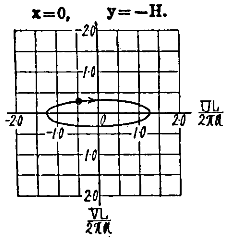

Fig. 57. $\frac{H}{L}=0{\cdot}25$,

x=0, y=0.

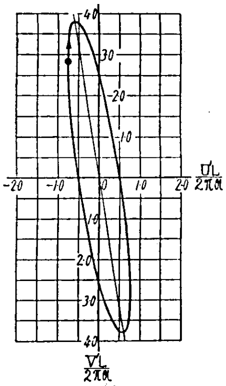

Fig. 58. $\frac{H}{L}=0{\cdot}26$,

x=0, y=−H.

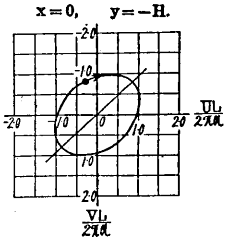

Fig. 59. $\frac{H}{L}=0{\cdot}26$,

x=0, y=0.

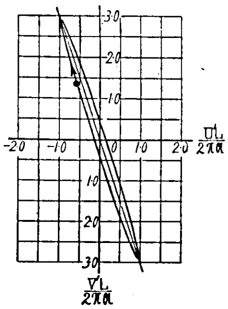

Fig. 60. $\frac{H}{L}=0{\cdot}27$,

x=0, y=−H.

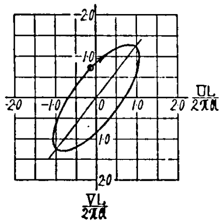

Fig. 61. $\frac{H}{L}=0{\cdot}27$,

x=0, y=0.

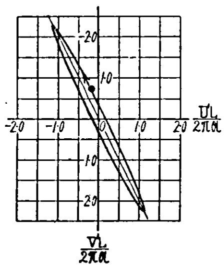

Fig. 62. $\frac{H}{L}=0{\cdot}28$,

x=0, y=−H.

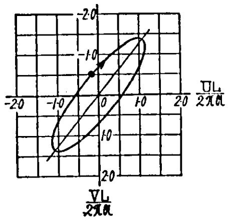

Fig. 63. $\frac{H}{L}=0.28$,

x=0, y=0.

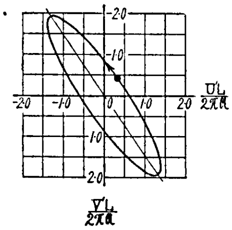

Fig. 64. $\frac{H}{L}=0{\cdot}29$,

x=0, y=−H.

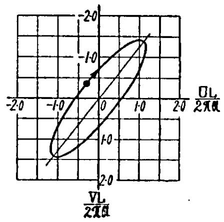

Fig. 65. $\frac{H}{L}=0{\cdot}29$,

x=0, y=0.

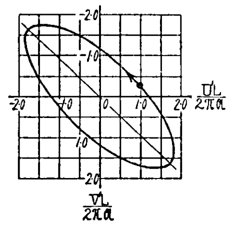

Fig. 66. $\frac{H}{L}=0{\cdot}30$,

x=0, y=−H.

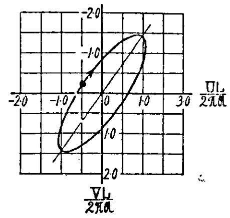

Fig. 67. $\frac{H}{L}=0{\cdot}30$,

x=0, y=0.

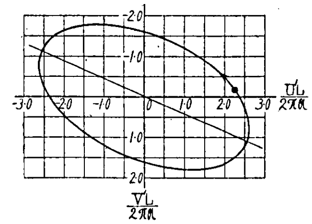

Fig. 68. $\frac{H}{L}=0{\cdot}31$,
x=0, y=−H.

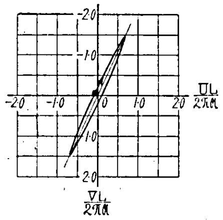

Fig. 69. $\frac{H}{L}=0{\cdot}31$,
x=0, y=0.

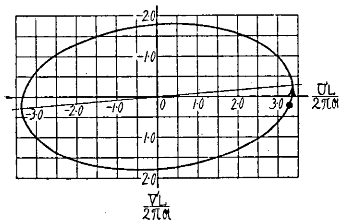

Fig. 70. $\frac{H}{L}=0{\cdot}32$,
x=0, y=−H.

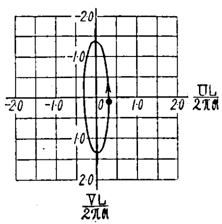

Fig. 71. $\frac{H}{L}=0{\cdot}32$,
x=0, y=0.

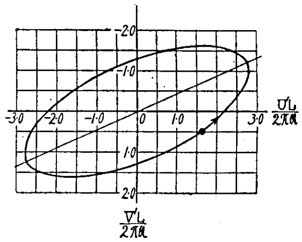

Fig. 72. $\frac{H}{L}=0{\cdot}33$,
x=0, y=−H.

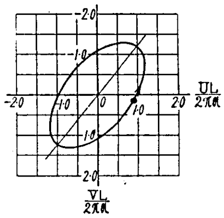

Fig. 73. $\frac{H}{L}=0{\cdot}33$,
x=0, y=0.

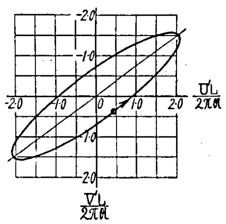

Fig. 74. $\frac{H}{L}=0{\cdot}34$,
x=0, y=−H.

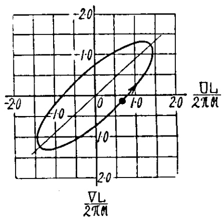

Fig. 75. $\frac{H}{L}=0{\cdot}34$,
x=0, y=0.

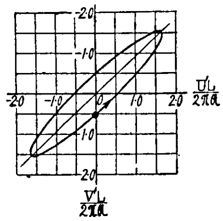

Fig. 76. $\frac{H}{L}=0{\cdot}35$,
x=0, y=−H.

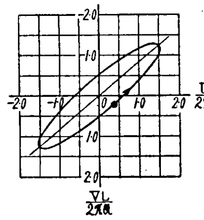

Fig. 77. $\frac{H}{L}=0{\cdot}35$,
x=0, y=0.

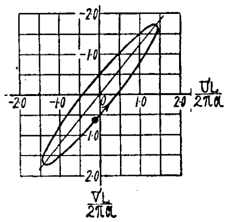

Fig. 78. $\frac{H}{L}=0{\cdot}36$,
x=0, y=−H.

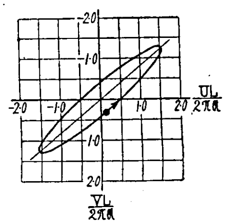

Fig. 79. $\frac{H}{L}=0{\cdot}36$,
x=0, y=0.

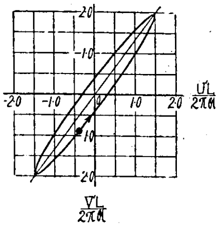

Fig. 80. $\frac{H}{L}=0{\cdot}37$,

$x=0$, $y=-H$.

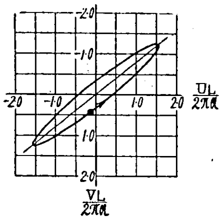

Fig. 81. $\frac{H}{L}=0{\cdot}37$,

$x=0$, $y=0$.

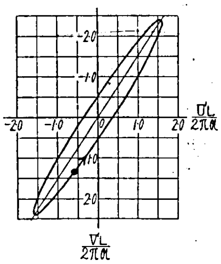

Fig. 82. $\frac{H}{L}=0{\cdot}38$,

$x=0$, $y=-H$.

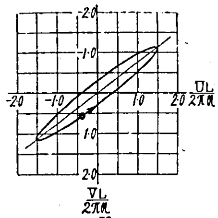

Fig. 83. $\frac{H}{L}=0{\cdot}38$,

$x=0$, $y=0$.

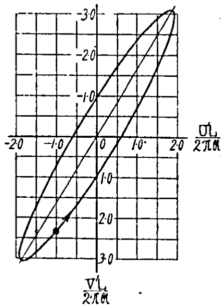

Fig. 84. $\frac{H}{L}=0{\cdot}39$,

$x=0$, $y=-H$.

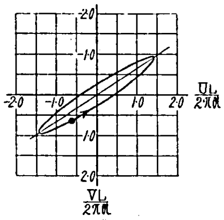

Fig. 85. $\frac{H}{L}=0.39$,

$x=0$, $y=0$.

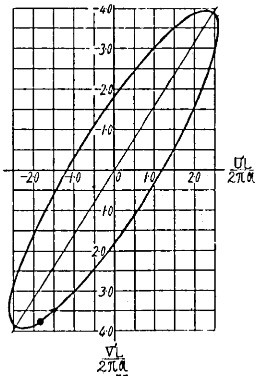

Fig. 86. $\frac{H}{L}=0{\cdot}40$,

$x=0$, $y=-H$.

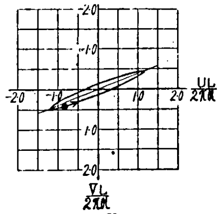

Fig. 87. $\frac{H}{L}=0{\cdot}40$,

$x=0$, $y=0$.

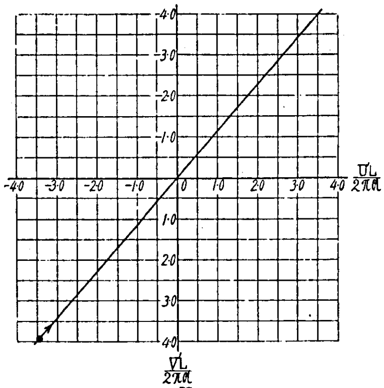

Fig. 88. $\frac{H}{L}=0{\cdot}41$,

$x=0$, $y=-H$.

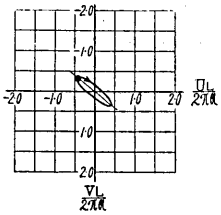

Fig. 89. $\frac{H}{L}=0{\cdot}41$,

$x=0$, $y=0$.

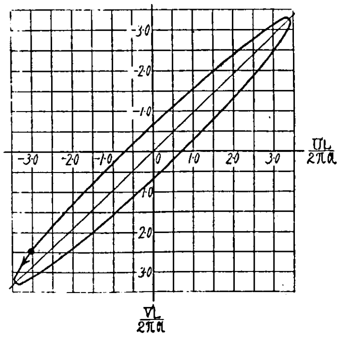

Fig. 90. $\frac{H}{L}=0{\cdot}42$,

$x=0$, $y=-H$.

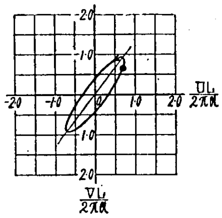

Fig. 91. $\frac{H}{L}=0{\cdot}42$,

$x=0$, $y=0$.

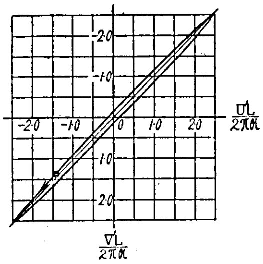

Fig. 92. $\frac{H}{L}=0{\cdot}43$, x=0, y=−H.

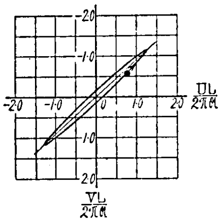

Fig. 93. $\frac{H}{L}=0{\cdot}43$, x=0, y=0.

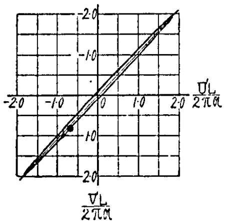

Fig. 94. $\frac{H}{L}=0{\cdot}44$, x=0, y=−H.

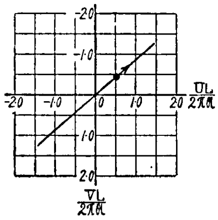

Fig. 95. $\frac{H}{L}=0{\cdot}44$, x=0, y=0.

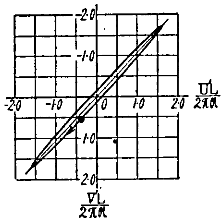

Fig. 96. $\frac{H}{L}=0{\cdot}45$, x=0, y=−H.

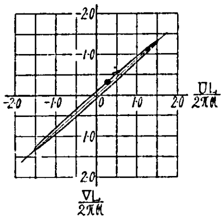

Fig. 97. $\frac{H}{L}=0{\cdot}45$, x=0, y=0.

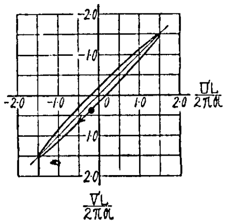

Fig. 98. $\frac{H}{L}=0{\cdot}46$, x=0, y=−H.

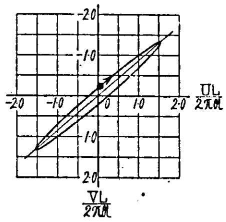

Fig. 99. $\frac{H}{L}=0{\cdot}46$, x=0, y=0.

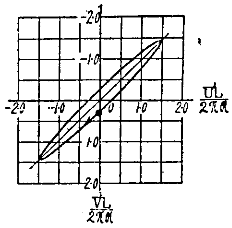

Fig. 100. $\frac{H}{L}=0{\cdot}47$, x=0, y=−H.

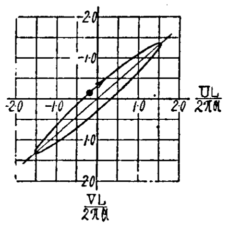

Fig. 101. $\frac{H}{L}=0{\cdot}47$, x=0, y=0.

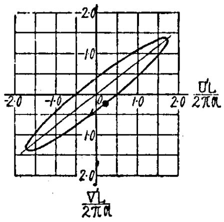

Fig. 102. $\frac{H}{L}=0{\cdot}48$, x=0, y=−H.

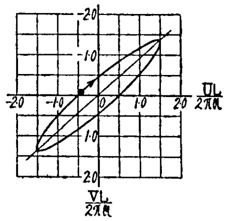

Fig. 103. $\frac{H}{L}=0{\cdot}48$, x=0, y=0.

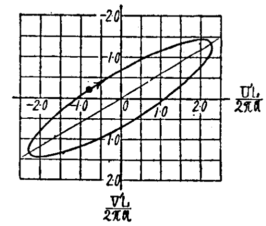

Fig. 104. $\frac{H}{L}=0{\cdot}49$,
$x=0, \quad y=-H.$

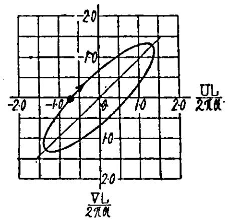

Fig. 105. $\frac{H}{L}=0{\cdot}49$,
$x=0, \quad y=0.$

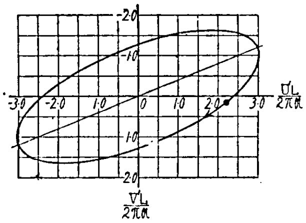

Fig. 106. $\frac{H}{L}=0{\cdot}50$,
$x=0, \quad y=-H.$

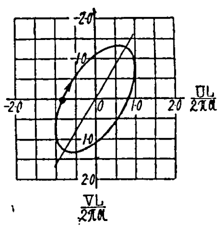

Fig. 107. $\frac{H}{L}=0{\cdot}50$,
$x=0, \quad y=0.$

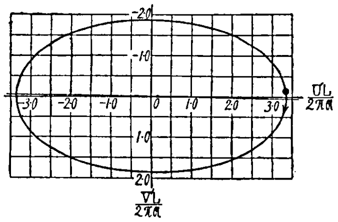

Fig. 108. $\frac{H}{L}=0{\cdot}51$,
$x=0, \quad y=-H.$

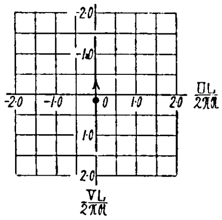

Fig. 109. $\frac{H}{L}=0{\cdot}51$,
$x=0, \quad y=0$

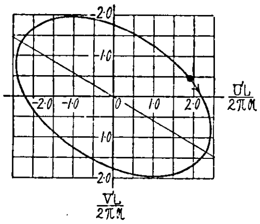

Fig. 110. $\frac{H}{L}=0{\cdot}52$,
$x=0, \quad y=-H.$

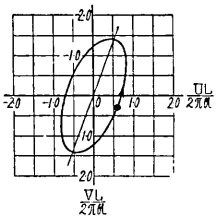

Fig. 111. $\frac{H}{L}=0{\cdot}52$,
$x=0, \quad y=0.$

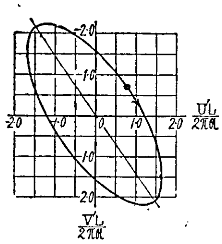

Fig. 112. $\frac{H}{L}=0{\cdot}53$,
$x=0, \quad y=-H.$

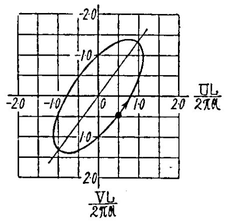

Fig. 113. $\frac{H}{L}=0{\cdot}53$,
$x=0, \quad y=0.$

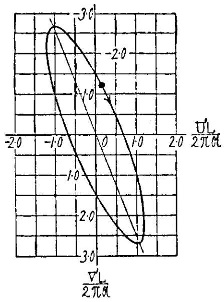

Fig. 114. $\frac{H}{L}=0{\cdot}54$,
$x=0, \quad y=-H.$

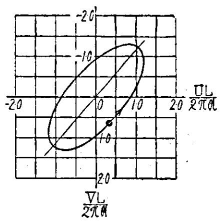

Fig. 115. $\frac{H}{L}=0{\cdot}54$,
$x=0, \quad y=0.$

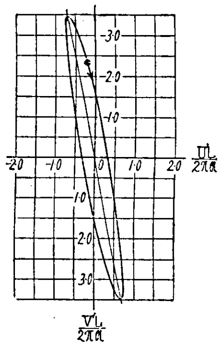

Fig. 116. $\frac{H}{L}=0{\cdot}55$.

x=0, y=−H.

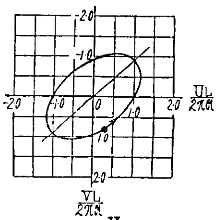

Fig. 117. $\frac{H}{L}=0{\cdot}55$,

x=0, y=0.

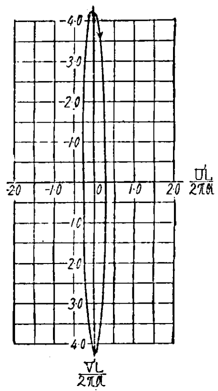

Fig. 118. $\frac{H}{L}=0{\cdot}56$,

x=0, y=−H.

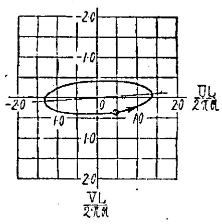

Fig. 119. $\frac{H}{L}=0{\cdot}56$,

x=0, y=0.

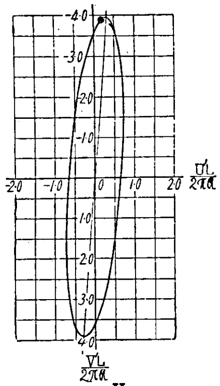

Fig. 120. $\frac{H}{L}=0{\cdot}57$,

x=0, y=−H.

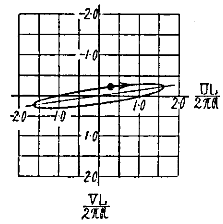

Fig. 121. $\frac{H}{L}=0{\cdot}57$,

x=0, y=0.

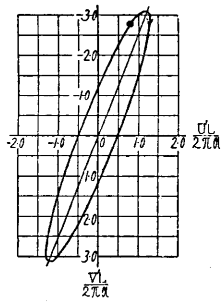

Fig. 122. $\frac{H}{L}=0{\cdot}58$,

x=0, y=−H.

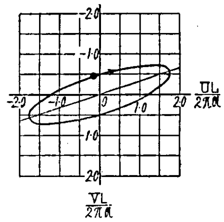

Fig. 123. $\frac{H}{L}=0{\cdot}58$,

x=0, y=0.

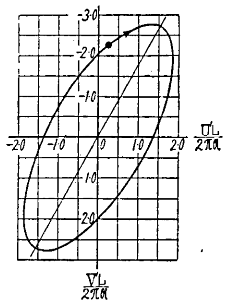

Fig. 124. $\frac{H}{L}=0{\cdot}59$,

x=0, y=−H.

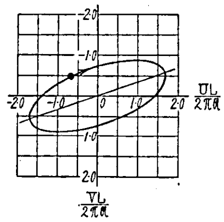

Fig. 125. $\frac{H}{L}=0{\cdot}59$,

x=0, y=0.

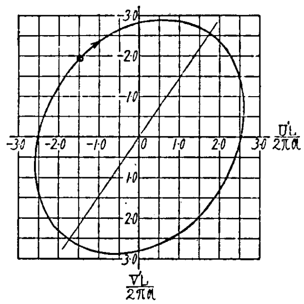

Fig. 126. $\frac{H}{L}=0{\cdot}60$,

x=0, y=−H.

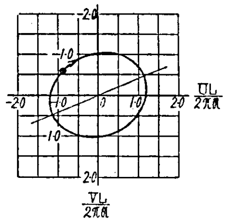

Fig. 127. $\frac{H}{L}=0{\cdot}60$,

x=0, y=0.

Upon comparing these figures with those obtained by K. Sezawa[12], it will be seen that the minor and major axes, their ratio, and the inclination angle of the elliptic orbit of the top surface particle in the surface layer in the present case of $\mu'/\mu=1.10$ have markedly larger fluctuations with respect to the variation in H/L than those in the case of $\mu'/\mu=1/2$. As already pointed out by Sezawa[13], these fluctuations of ξ, η and η/ξ or τ may be caused by interference effects of the reflected and refracted waves in the surface layer, while the fact that fluctuations in the case of $\mu'/\mu=1/10$ become larger than those in the case of $\mu'/\mu=1/2$ may mainly be caused by the fact that the selective resonance in the surface layer in the former case becomes markedly more effective than in the latter. The resonance phenomena in the surface layer will be discussed in the next chapter.

We calculated the types of orbital motions on the free and the bottom surfaces of the surface layer for the respective cases of H/L in the present example, the results being shown in Fig. 8～127. In these figures, the emergent angle of the primary wave in the subjacent medium is always 45° at the lower boundary of the surface layer. It will be seen on comparing these figures, that the minor and major axes, their ratio, and the inclination angle which the major axis makes with the horizontal surface fluctuate markedly with respect to the variation in H/L.

Chapter II. Resonance Phenomenon in the Surface Layer.

We have already calculated the forced stationary vibrations (horizontal and vertical) on the free surface of the surface layer when a dilatational harmonic wave of infinite extent is obliquely incident on the bottom surface of the stratum, being expressed by (40) and (41), namely,

$$\left.\frac{LU'}{2\pi a}\right]_{\substack{y=-H\\x=0}}=\sqrt{\alpha^2+\beta^2}\,\sin\left\{z+\tan^{-1}\frac{\beta}{\alpha}\right\}, \tag{40'}$$

$$\left.\frac{LV'}{2\pi a}\right]_{\substack{y=-H\\x=0}}=\sqrt{\alpha'^2+\beta'^2}\,\sin\left\{z+\tan^{-1}\frac{\beta'}{\alpha'}\right\}, \tag{41'}$$

in which a and b become $19{\cdot}3657\,H/L$ and $34{\cdot}1264\,H/L$ respectively. If we numerically calculate the amplitudes of the forced vibrations expressed by (40) and (41) with the respective values of H/L, we get Table IV, the results being shown in Figs. 128, 129. Phase-differences $\tan^{-1}\beta/\alpha$

12) K. SEZAWA and K. KANAI, *Bull. Earthq. Res. Inst.*, **12** (1934), 269.
13) K. SEZAWA and K. KANAI, *loc. cit.*

and $\tan^{-1}\beta'/\alpha'$ are also shown in Table IV.

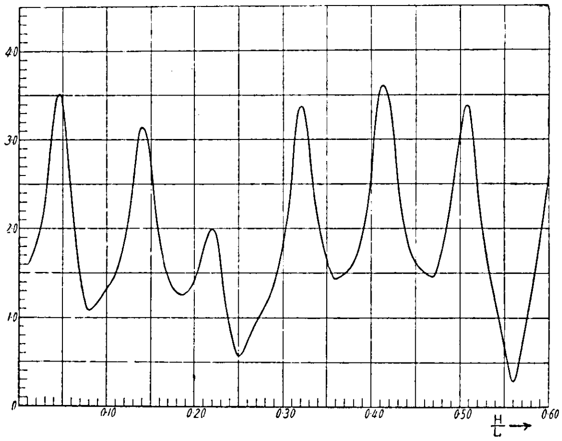

Fig. 128. Resonance curve of horizontal vibration. (Horizontal displacement amplitude of the particle on the top surface of the surface layer.)

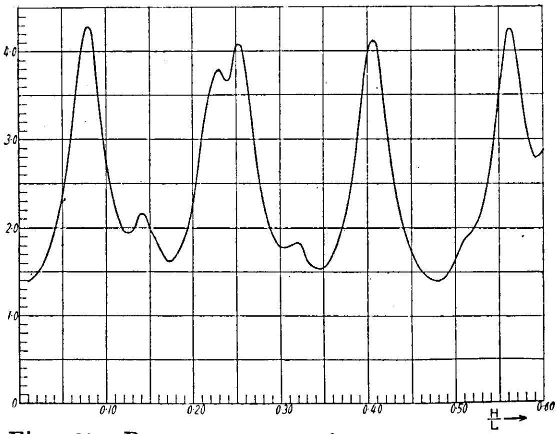

Fig. 129. Resonance curve of vertical vibration. (Vertical displacement amplitude of the particle on the top surface of the surface layer.)

Table IV.

$\frac{H}{L}$	Horizontal amplitude	Vertical amplitude	$\tan^{-1}\frac{\beta}{\alpha}$	$\tan^{-1}\frac{\beta'}{\alpha'}$
0·01	1·59	1·3 7	3·03	3·09
0·02	1·838	1·470	2·895	3·05
0·03	2·356	1·632	2·662	2·914
0·04	3·227	1·93	2·201	2·914
0·05	3·410	2·88	1·431	2·821

(to be continued.)

Table IV. (*continued.*)

$\frac{H}{L}$	Horizontal amplitude	Vertical amplitude	$\tan^{-1}\frac{\beta}{\alpha}$	$\tan^{-1}\frac{\beta'}{\alpha'}$
0·06	2·340	3·004	0·825	2·522
0·07	1·482	3·86	0·544	2·160
0·08	1·080	4·552	0·614	1·915
0·09	1·169	3·59	0·641	1·102
0·10	1·248	2·743	0·489	0·813
0·11	1·474	2·220	0·298	0·670
0·12	1·873	1·957	0·0327	0·605
0·13	3·517	1·957	2·767	0·555
0·14	5·145	2·162	2·05	0·356
0·15	2·680	1·975	1·269	0·0819
0·16	1·880	1·81	0·717	3·06
0·17	1·456	1·633	0·350	3·0
0·18	1·279	1·682	0·0254	3·04
0·19	1·265	1·866	2·821	3·00
0·20	1·414	2·247	2·393	2·937
0·21	1·750	3·012	1·780	2·743
0·22	1·994	3·55	0·930	2·344
0·23	1·531	3·78	2·936	1·929
0·24	0·938	3·660	1·893	1·734
0·25	0·567	4·174	0·209	1·346
0·26	0·753	3·832	1·541	0·832
0·27	0·966	2·927	0·638	0·492
0·28	1·124	2·300	0·134	0·322
0·29	1·380	1·943	2·913	0·225
0·30	1·824	1·78	2·567	0·163
0·31	2·620	1·794	2·103	0·0894
0·32	3·38	1·830	1·350	3·03
0·33	2·812	1·630	0·617	2·863
0·34	2·08	2·02	0·213	2·905
0·35	1·682	1·542	3·130	2·797
0·36	1·44	1·690	3·060	2·753
0·37	1·492	1·950	2·874	2·677
0·38	1·61	2·403	2·759	2·539
0·39	1·925	3·103	2·611	2 301
0·40	2·59	3·97	2·358	1·883
0·41	3·580	4·09	1·830	1·303
0·42	3·400	3·27	1·079	0·840
0·43	2·473	2·503	0·610	0·574
0·44	1 88	2·015	0·372	0·418

(*to be continued.*)

Table IV. (*continued*)

$\frac{H}{L}$	Horizontal amplitude	Vertical amplitude	$\tan^{-1}\frac{\beta}{\alpha}$	$\tan^{-1}\frac{\beta'}{\alpha'}$
0·45	1·605	1·710	0·239	0·314
0·46	1·52	1·534	0·132	0·252
0·47	1·455	1·431	0·0249	0·203
0·48	1·77	1·40	3·02	0·173
0·49	2·297	1·449	0·787	0·144
0·50	3·054	1·626	2·339	0·0928
0·51	3·380	1·873	1·496	3·070
0·52	2·453	1·958	0·890	2·918
0·53	1·670	2·190	0·470	2·817
0·54	1·180	2·680	0·126	2·671
0·55	0·738	3·480	0·867	2·404
0·56	0·292	4·237	0·677	1·852
0·57	0·701	3·950	0·134	1·402
0·58	1·268	3·145	2·546	1·088
0·59	1·854	2·788		0·943
0·60	2·60	2·90		0·740
0·62	1·855	2·120	——	0·142

Taking next the real parts only, we easily get the stationary vibrations of the bottom surface of the surface layer from expressions (15) and (16) as follows:

$$\frac{UL}{2\pi a}\Big]_{\substack{y=0\\x=0}} = \cos\theta\sqrt{\left(1+A'+B'\right)^2+\left(A''+\frac{s}{f}B''\right)^2}\sin(z+\alpha)\,, \tag{50}$$

$$\frac{VL}{2\pi a}\Big]_{\substack{y=0\\x=0}} = \cos\theta\sqrt{\left(-\frac{r}{f}+\frac{r}{f}A'-B'\right)^2+\left(B''-\frac{r}{f}A''\right)^2}\sin(z+\alpha')\,, \tag{51}$$

where

$$\alpha=\tan^{-1}\left\{\frac{-\left(A''+\frac{s}{f}B''\right)}{\left(1+A'+\frac{s}{f}B'\right)}\right\}, \tag{52}$$

$$\alpha'=\tan^{-1}\left\{\frac{\left(B''-\frac{r}{f}A''\right)}{\left(-\frac{r}{f}+\frac{r}{f}A'-B'\right)}\right\}, \tag{53}$$

and $\cos\theta=0{\cdot}7071$. Obviously α and α' should be taken satisfying

$$\left.\begin{aligned}\sqrt{\left(1+A'+\frac{s}{f}B'\right)^2+\left(A''+\frac{s}{f}B''\right)^2}\sin\alpha=-\left(A''+\frac{s}{f}B''\right),\\ \sqrt{\left(1+A'+\frac{s}{f}B'\right)^2+\left(A''+\frac{s}{f}B''\right)^2}\cos\alpha=1+A'+\frac{s}{f}B',\end{aligned}\right\}$$

$$\left.\begin{aligned}\sqrt{\left(-\frac{r}{f}+\frac{r}{f}A'-B'\right)^2+\left(B''-\frac{r}{f}A''\right)^2}\sin\alpha'=\left(B''-\frac{r}{f}A''\right),\\ \sqrt{\left(-\frac{r}{f}+\frac{r}{f}A'-B'\right)^2+\left(B''-\frac{r}{f}A''\right)^2}\cos\alpha'=\left(-\frac{r}{f}+\frac{r}{f}A'-B'\right).\end{aligned}\right\}$$

In these expressions, A', A'' and B', B'' are the real and the imaginary parts of A and B such that

$$A=A'+iA'', \qquad B=B'+iB'', \tag{54}$$

the values of which are given in Table I with the respective values of H/L when $\rho=\rho'$, $\lambda=\mu$, $\lambda'=\mu'$, $\theta=45°$, $\mu'/\mu=1/10$. In the present actual case, we calculated the amplitudes of the forced stationary vibrations (horizontal and vertical) at the bottom surface of the surface layer (shown in Table V), the phase-differences α and α' being also calculated. Figs. 130, 131 show the amplitudes (horizontal and vertical) of the bottom surface of the surface layer.

Table V.

$\frac{H}{L}$	Horizontal amplitude	Vertical amplitude	α	α'
0·01	1·491	1·358	2·996	3·080
0·02	1·457	1·347	2·817	3·020
0·03	1·330	1·327	2·548	2·952
0·04	0·847	1·302	2·035	2·875
0·05	0·219	1·271	1·623	2·749
0·06	0·937	1·157	0·815	2·516
0·07	1·195	0·785	0·550	2·155
0·08	1 415	0·0714	0·414	2·504
0·09	1·594	0·650	0·227	0·890
0·10	1·654	0·989	0·0385	0·597
0·11	1·647	1·120	2·185	0·422
0·12	1·605	1·170	2·784	0·320
0·13	1·398	1·191	2·444	0·288
0·14	0·652	1·310	1·906	0·300
0·15	0·433	1·460	0·730	0·183

(*to be continued.*)

Table V. (*continued*)

$\frac{H}{L}$	Horizontal amplitude	Vertical amplitude	a	a'
0·16	0·978	1·493	0·453	0·0591
0·17	1·154	1·490	0·237	3·10
0·18	1·194	1·481	0·0798	3·02
0·19	1·1425	1·476	3·075	2·922
0·20	0·983	1·450	2·982	2·785
0·21	0·659	1·350	0·706	2·288
0·22	0·960	0·982	3·135	2·548
0·23	1·672	0·573		
0·24	1·770	0·336		
0·25	1·460	0·315		
0·26	1·037	0·975	2·871	0·953
0·27	1·065	1·289	3·01	0·393
0·28	1·160	1·395		
0·30	1·064	1·464	2·671	0·143
0·31	0·676	1·455	3·03	0·0321
0·32	0·302	1·388	1·514	3·065
0·33	1·185	1·305	0·852	3·05
0·34	1·470	1·30	0·462	3·025
0·35	1·550	1·30	0·235	2·974
0·36	1·570	1·285	0·0713	2·899
0·37	1·562	1·245	3·06	2·796
0·38	1·510	1·146	2·904	2·647
0·39	1·434	0·941	2·692	2·408
0·40	1·168	0·443	2·339	2·056
0·41	0·441	0·362	1·567	1·127
0·42	0·719	0·906	1·248	0·783
0·43	1·267	1·150	0·654	0·529
0·44	1·445	1·255	0·362	0·366
0·45	1·513	1·310	0·175	0·256
0·46	1·535	1·330	0·0264	0·172
0·47	1·530	1·340	3·03	0·103
0·48	1·498	1·340	2·851	0·0462
0·49	1·387	1·332	2·599	3·130
0·50	0·997	1·335	2·139	3·116
0·51	0·0240	1·402	2·452	3·06
0·52	0·837	1·427	0·787	2·939
0·53	1·110	1·388	0·449	2·80
0·54	0·714	1·297	0·487	2·616
0·55	1·160	1·067	0·260	2·326

(*to be continued.*)

Table V. (*continued*)

$\frac{H}{L}$	Horizontal amplitude	Vertical amplitude	a	a'
0·56	1·3475	0·3885	0·323	1·608
0·57	1·644	0·2852	0·173	0·851
0·58	1·760	0·710	3·05	0·679
0·59	1·690	0·874	2·734	0·562
0·60	1·184	1·037	2·294	0·604

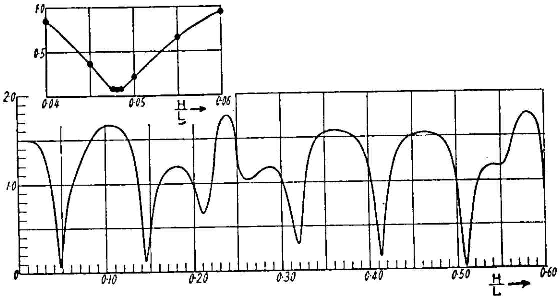

Fig. 130. Horizontal displacement amplitude of the particle on the bottom surface of the surface layer.

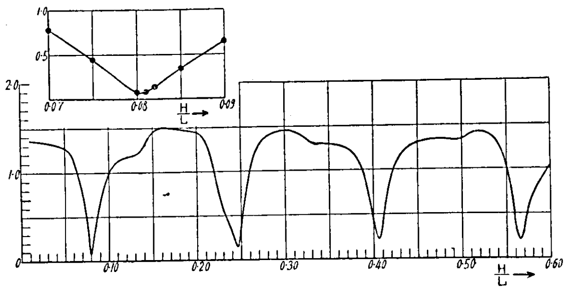

Fig. 131. Vertical displacement amplitude of the particle on the bottom surface of the surface layer.

It will be seen from Figs. 128, 129, 130, and 131 that the horizontal and the vertical vibration amplitudes on the top surface are usually larger than the respective amplitudes on the bottom surface of the surface stratum. It will be seen, moreover, that the respective positions of the maxima and minima of the horizontal (or vertical) vibration amplitudes with respect to the same values of H/L are completely changed in both amplitudes on the top surface and those on the bottom surface of the surface stratum. Generally speaking, the amplitude at the bottom surface of the surface layer becomes minimum and very small for the values of H/L, for which the amplitude on the top surface of the surface layer becomes maximum and very large. It is clear that the curves shown in Figs. 128, 129 are *resonance curves* of the vibrations (horizontal and vertical) of the surface stratum. And it will be seen from Figs. 128, 129 that the amplitudes of the forced oscillation at the top surface of the surface layer become relatively large at such periods as are synchronous successively with the resonance periods of vibration of the surface stratum. These resonance periods of oscil-

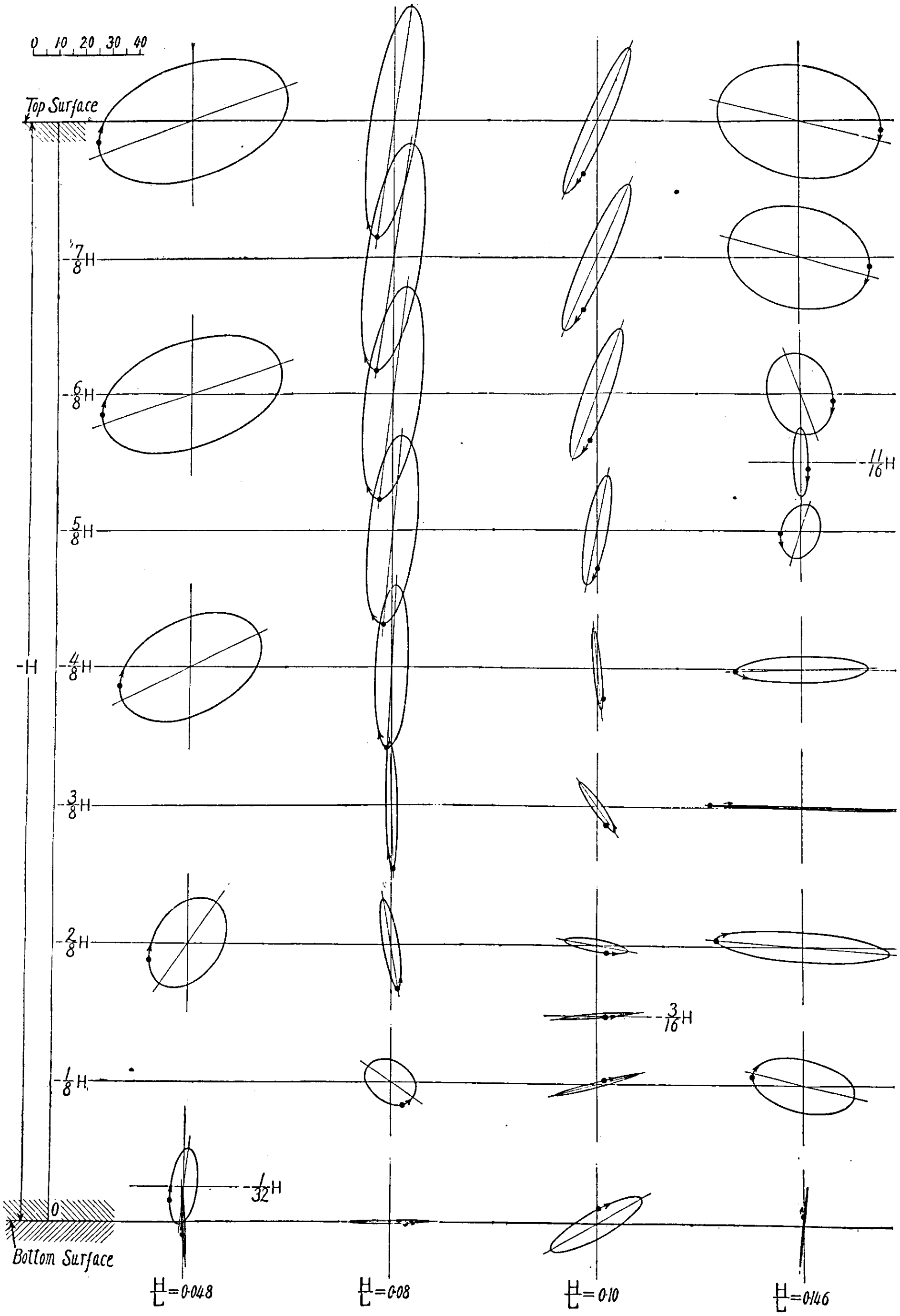
0 10 20 30 40
Top Surface
-7/8 H
-6/8 H
-5/8 H
-4/8 H
-H
-3/8 H
-2/8 H
-1/8 H
-11/16 H
-3/16 H
-1/32 H
0
Bottom Surface
H/L=0·048
H/L=0·08
H/L=0·10
H/L=0·146

Fig. 132.

lation of the surface stratum usually differ in their horizontal and vertical vibrations as may be seen in Figs. 128, 129. The curves shown in Figs. 128, 129 are not regular as in the resonance curves when the primary waves are vertically upward incident on the bottom surface of the surface layer[14].

When the primary wave is vertically upward and incident on the bottom surface of the surface layer, and the periods of the primary incident wave become synchronous with the resonance periods of oscillation of the surface stratum, the bottom surface of the surface layer should become a nodal plane[15], that is, the displacements of particles on the bottom surface of the surface layer become zero. This fact, however, may not necessarily obtain when the primary wave is obliquely incident on the bottom surface of the surface layer, as may be seen from Figs. 130 and 131. It is noteworthy, moreover, that the fundamental resonance period of oscillation of the horizontal seismal vibration becomes longer than that of the vertical seismal vibration, and that in the case of horizontal vibration the ratio of the resonance period of higher order to the fundamental one tends to become larger than the ratio of the resonance period of the same higher order to the fundamental one in the case of vertical vibration, as may also be seen from Figs. 130 and 131. The resonance curves in Figs. 130 and 131 show that the amplitudes of the horizontal vibration usually become smaller than those of the vertical one, as may conspicuously be seen in resonance conditions.

Calculating from expressions (40) and (41) the vibrational movements of particles in the surface stratum, we obtain Fig. 132 which shows the elliptic orbits of particles on surfaces $y=0$, $y=\frac{1}{8}H$, $y=-\frac{2}{8}H$, $y=-\frac{3}{8}H$, $y=-\frac{4}{8}H$, $y=-\frac{5}{8}H$, $y=-\frac{6}{8}H$, $y=-\frac{7}{8}H$, and $y=-H$ when $H/L=0{\cdot}048$, $0{\cdot}080$, $0{\cdot}100$ and $0{\cdot}145$ respectively. Of course, in Fig. 132, the cases of $H/L=0{\cdot}048$ and $H/L=0{\cdot}145$ correspond to the movements of particles in the surface layer when the periods of the primary incident wave become equal to the fundamental and the second resonance periods of horizontal vibrations in the surface layer respectively, and the case of $H/L=0{\cdot}080$ corresponds to the movement of particles in the surface stratum when the period of the primary incident wave becomes equal to the fundamental resonance period of vertical vibration of the surface stratum. The horizontal movements of particles in the surface

14) K. SEZAWA and K. KANAI, *loc. cit.*

15) K. SEZAWA and K. KANAI, *loc. cit.*

layer when $H/L=0{\cdot}048$, $0{\cdot}080$, $0{\cdot}100$ and $0{\cdot}145$ are shown in Figs. 133, 134, 135 and 136 respectively[16]. It will be seen from Figs. 132~136

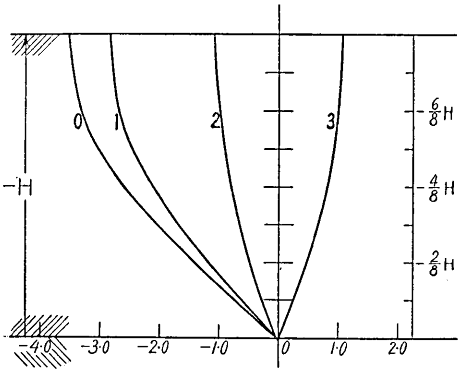

Fig. 133. Horizontal displacement in the surface layer when $H/L=0{\cdot}048$.

0: $\frac{t}{T}=0$, 1: $\frac{t}{T}=2{\cdot}2$, 2: $\frac{t}{T}=0{\cdot}4$,

3: $\frac{t}{T}=0{\cdot}7$.

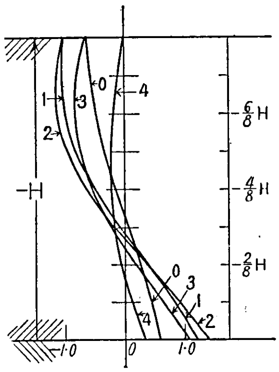

Fig. 134. Horizontal displacement in the surface layer when $H/L=0{\cdot}08$.

0: $\frac{t}{T}=0$, 1: $\frac{t}{T}=0{\cdot}2$, 2: $\frac{t}{T}=0{\cdot}3$,

3: $\frac{t}{T}=0{\cdot}4$, 4: $\frac{t}{T}=0{\cdot}5$.

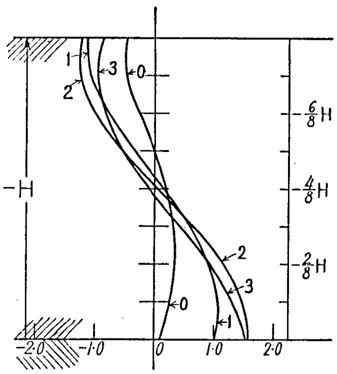

Fig. 135. Horizontal displacement in the surface layer when $H/L=0{\cdot}100$.

0: $\frac{t}{T}=0$, 1: $\frac{t}{T}=0{\cdot}2$, 2: $\frac{t}{T}=0{\cdot}3$,

3: $\frac{t}{T}=0{\cdot}4$.

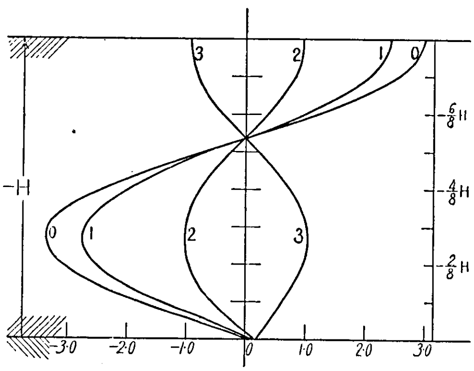

Fig. 136. Horizontal displacement in the surface layer when $H/L=0{\cdot}145$.

0: $\frac{t}{T}=0$, 1: $\frac{t}{T}=0{\cdot}2$, 2: $\frac{t}{T}=0{\cdot}3$,

3: $\frac{t}{T}=0{\cdot}4$.

that even if the period of the primary incident wave becomes synchronous with the resonance periods (of horizontal and vertical vibrations) of the surface layer, the amplitudes of displacement (of horizontal and vertical vibrations) do not become infinite as in the case of an isolated elastic pendulum. It will be seen, moreover, that the vibration modes

16) To obtain the results shown in Figs. 132~136, we used expressions (44) and (45).

(of horizontal and vertical vibrations) in the resonance conditions do not necessarily become equal to the free vibration modes that may be excited in the surface layer when it may be assumed as an isolated elastic pendulum. It may be worth noticing, furthermore, that the resonance periods of the vibrations (horizontal and vertical) of the surface stratum are not constant, but depend upon the angle of incidence of the primary wave at the bottom surface of the surface layer. From Figs. 130 and 131, we can get the resonance periods of vibration when the incidence angle of the primary dilatational wave becomes 45°, as shown in Table VI. If then the wave velocity V_1 of the dilatational wave in the subjacent medium and also the period T of the primary incident dilatational wave are known, the resonance periods of vibration of the surface stratum in an actual case can easily be determined by the values shown in Table V and by the relation $L=V_1T$, when the angle of incidence of the primary wave becomes 45°.

Table VIa. Resonance Periods of Horizontal Vibration.

1st	2nd
$0{\cdot}048\,H/L$	$0{\cdot}145\,H/L$

Table VIb. Resonance Periods of Vertical Vibration.

1st	2nd
$0{\cdot}08\,H/L$	$0{\cdot}245\,H/L$

Recently T. Saita[17] and M. Suzuki studied the seismal vibrations at Marunouti, Tokyo, Japan. The English abstract of their paper in Japanese reads as follows:

Lately the authors have observed seismic disturbances at Marunouchi where is the representative ground of the down town in Tokyo. These observations were held at the same time in three places; which are surface ground, 30 feet and 68 feet deep underground respectively. The 68 feet deep underground level is exactly the boundary of alluvium and diluvium. The diluvium is made of compact materials and its bearing power is greater than 20 tons per square foot, while the alluvium is made of soft materials and its bearing power is less than 1 ton per square foot. Therefore, these observations have determined how 68 feet thick soft alluvial layer vibrates by seismic disturbances. The instruments were Ishimoto's seismic accelerometers. The authors have found that, in alluvial layer, there are numerous waves having about 0·2 sec. and 0·7 sec. periods; in diluvial formation, 0·25 sec. and 0·45 sec. respectively. In consequence of drawing the resonance curve for vibrations in the alluvium, the author are able to ascertain that 0·25 sec. and 0·75 sec. are the proper periods of the alluvial layer. Moreover, the acceleration in 68 feet deep undreground was about 1/3 to 1/5 of the surface ground. These data will be available to engineering seismology and prevention of earthquake disaster.

The amplitude ratio curve obtained by them is shown in Fig. 137,

17) T. SAITA and M. SUZUKI, "On the Upper Surface and Underground Seismic Disturbances at the Down Town in Tokyo," *Bull. Earthq. Res. Inst.*, **12** (1934), 517.

in which the abscissa corresponds to the vibration period of the alluvium surface layer and the ordinate shows the ratio of the horizontal accerelation amplitudes at the top surface to those 68 feet underground. We do not know, however, the angle of incidence of the seismic waves at the bottom surface of the alluvium surface layer or the particular kind of incident seismic wave referred to in Saita's data of observations, so that our mathematical results may not be theoretically applicable to Saita's observation. But if we assume that the acceleration in Saita's data is of harmonic type, it is possible to say that the ratios of the maximum horizontal displacement amplitudes at the top surface to those at the bottom surface, which are shown respectively in Figs. 128 and 130, become approximately the same as the actual ratios of the large horizontal accelerations at the top surface to those at the bottom surface of the alluvium layer in Saita's data. The values of the actual ratios obtained by Saita are from about 1/3 to 1/5 as mentioned in his paper. By calculating the ratio of the displacement amplitudes on the top to those on the bottom surfaces with the respective values of H/L from Table III and IV, we get Table VII in which the ratios are given, the results being shown in Figs. 138 and 139. Fig. 138 corresponds to the horizontal displacement amplitude ratio and Fig. 139 shows the vertical displacement amplitude ratio. If we compare next the amplitude ratio curve in Fig. 138 with

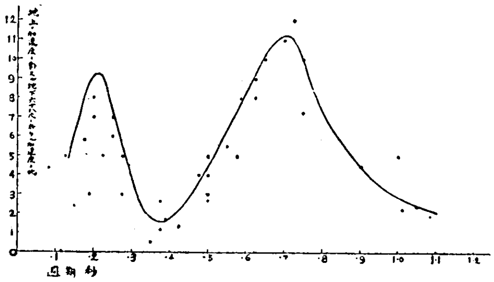

Fig. 137. Horizontal acceleration amplitude ratio obtained by T. Saita and M. Suzuki.

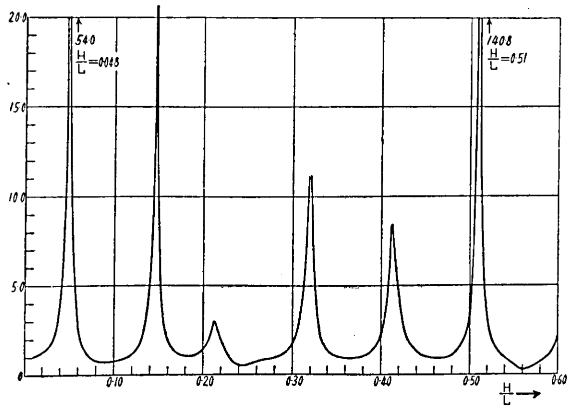

Fig. 138. Horizontal displacement amplitude ratio.

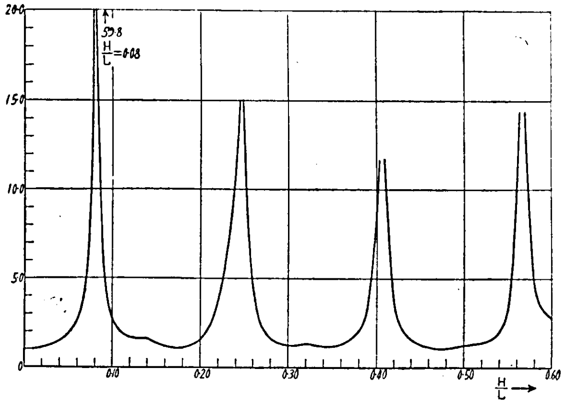

Fig. 139. Vertical displacement amplitude ratio.

Table VII.

$\frac{H}{L}$	Horizontal displacement amplitude ratio	Vertical displacement amplitude ratio	$\frac{H}{L}$	Horizontal displacement amplitude ratio	Vertical displacement amplitude ratio
0·01	1·066	1·022	0·32	11·20	1·318
0·02	1·1675	1·091	0·33	2·373	1·250
0·03	1·771	1·230	0·34	1·415	1·554
0·04	3·810	1·482	0·35	1·085	1·186
0·05	15·552	2·265	0·36	0·917	1·315
0·06	2·498	2·597	0·37	0·956	1·566
0·07	1·240	4·918	0·38	1·066	2·096
0·08	0·764	3·754	0·39	1·342	3·295
0·09	0·734	5·511	0·40	2·22	8·96
0·10	0·755	2·775	0·41	8·120	11·28
0·11	0·895	1·982	0·42	4·786	3·610
0·12	1·167	1·672	0·43	1·952	2·173
0·13	1·799	1·642	0·44	1·301	1·605
0·14	4·825	1·650	0·45	1·061	1·305
0·15	6·200	1·352	0·46	0·990	1·154
0·16	1·923	1·212	0·47	0·951	1·067
0·17	1·262	1·096	0·48	1·181	1·045
0·18	1·071	1·135	0·49	1·655	1·137
0·19	1·1075	1·264	0·50	3·064	1·219
0·20	1·438	1·550	0·51	1·408	1·336
0·21	2·655	2·231	0·52	2·930	1·373
0·22	2·076	3·616	0·53	1·550	1·577
0·23	0·917	6·600	0·54	1·652	2·065
0·24	0·529	10·90	0·55	0·636	3·262
0·25	0·479	13·25	0·56	0·217	10·90
0·26	0·726	3·932	0·57	0·427	13·85
0·28	0·969	1·649	0·58	0·721	4·430
0·30	1·715	1·215	0·59	1·097	3·190
0·31	3·861	1·232	0·60	2·195	2·798

that in Fig. 137, it will be seen that the first and second resonances in Fig. 138 correspond very roughly to the maxima at 0·7 sec. and 0·2 sec. respectively in Fig. 137. Since Saita has obtained only the amplitude ratio curve shown in Fig. 137, and has not shown the resonance curve[18] such as that shown in Fig. 138. It is impossible theoretically to compare Fig. 138, which is obtained from the resonance curve in Fig. 128, with the amplitude ratio curve in Fig. 137 obtained by Saita, with the result that we assume here that when the resonance curve is constructed from Saita's actual data, the resonance periods of Marunouti ground will work out to about 0·7 sec. and 0·2 sec. The magnitudes of these amplitude ratios at the respective resonances are then not strictly the same in Figs. 137 and 138. The ratio of the abscissa, at which the first maximum occurs, to that which gives the second maximum in Fig. 138, is about 3, the same ratio in Fig. 137 being about 3·5. These two values are also approximately equal in the two cases, that is, our mathematical results and Saita's experimental results.

From the foregoing discussion, it may be said that it will be in order to use the mathematical results in the present paper for obtaining the wave velocity of the dilatational wave in the diluvium lying under a top surface 20 m. thick at Marunouti. Therefore, using the value of the abscissa which gives the first maximum of the amplitude ratio in Fig. 138, such that

$$\frac{H}{L}=\frac{H}{V_1 T}=0{\cdot}048\,,$$

and the assumed resonance period of 0·7 sec. in Fig. 138, we get

$$\frac{H}{V_1\times 0{\cdot}7}=0{\cdot}048\,,\quad \text{or}\quad V_1 \doteqdot 570\ \text{m/s}\,,$$

assuming that the thickness of the alluvium at Marunouti is 20 meters, and the densities of the alluvium and diluvium are the same there.

Conclusion.

The present paper is a study of the forced stationary vibration of a surface stratum when a dilatational wave of harmonic type of in-

18) Saita has not shown in his paper the resonance curve of the horizontal seismal vibration of the surface stratum of alluvium, but he informed the present authors that he had also obtained it.

finite extent is obliquely incident on the bottom surface of the surface layer, therefore showing that there are resonance periods of oscillation in the surface layer. The amplitudes (horizontal and vertical) of the forced oscillations at the top surface of the surface layer become of course relatively large at such periods as are synchronous successively with the resonance periods of vibration of the surface layer. These resonance periods of oscillation of the surface stratum usually differ in their horizontal and vertical vibrations, and the fundamental resonance period of oscillation of the horizontal vibration becomes longer than that of the vertical vibration. When the primary wave is obliquely incident on the bottom surface of the surface layer, and the periods of the primary incident wave become synchronous with the resonance periods of oscillation of the surface layer, the bottom surface of the surface layer does not become necessarily a nodal plane of oscillation, as in the case when the primary wave is vertically upward and incident on the bottom surface of the surface layer. The forced vibration modes of horizontal and vertical vibrations of the surface layer in resonance condition do not necessarily become equal to the free vibration modes that may be excited in the surface layer, when it may be assumed to be an isolated elastic pendulum. Even if the period of the primary incident wave becomes synchronous with the resonance periods (of horizontal and vertical oscillations) of the surface layer, the displacement amplitudes (of horizontal and vertical vibrations) do not become infinite as in the case of the isolated elastic pendulum. It is noteworthy, moreover, that the resonance periods of vibrations (horizontal and vertical) of the surface layer are not constant, but depend upon the angle of incidence of the primary wave at the bottom surface of the surface layer.

We are yet unable theoretically to deal with the predominating periods in the surface layer in the seismal disturbance, which have an important connection with the prevention of earthquake disasters. It is our intention, on the next occasion, to study the predominating periods in the surface layer in a seismal disturbance by using the mathematical results given in the second chapter[19] of the previous paper. The wave phenomena in the surface layer when distortional waves of both finite and infinite extents are obliquely incident on the bottom of the surface layer having now been brought under mathematical treatment, the full results will be made available in the near future.

19) G. NISHIMURA, *loc. cit.*

The present authors wish to express their sincere thanks to Professor K. Sezawa for his interest and kind guidance in the course of the present study.

25. 斜めの入射波による表面層の振動とその共振れ性質

地震研究所 西村源六郎
高山威雄

前論文[1]の續報である本論文では具體的の例に就て數計算を行ひ，地表層に共振れ振動週期のある事を知つた．この週期は地表層の所謂固有週期と言つてよいかも知れないが，表面層に入射する强制波の入射角によつて異つた値をとるものである．この共振れ週期で表面層の振動を起しても表面層の振幅は無限大にならない事は勿論であるが，その振動の Mode は必ずしも表面層だけを彈性振子と考へた場合の自己振動の mode と一致しない事は注意を要す．齋田氏等[2]の求めた丸ノ內での水平加速度振幅の觀測結果に對する解釋に就ては彈性振子的な考の基でこれを處理してゐる樣であるが，著者達は次に發表する事にしてゐる表面層內に於ける free waves の問題を解決し，以つて forced waves に關する本論文より得た結果とを適當に組合せて，表面層の振動問題を解決してみたいと考へてゐる．

1) 西村源六郎 地震研究所彙報 **13** (1935), 540〜554.
2) 齋田時太郎，鈴木正治 地震研究所彙報 **12** (1934), 517.